Liver-Selective Glucocorticoid Antagonists: A Novel Treatment for Type 2 Diabetes

Thomas W. von Geldern,* Noah Tu,‖ Philip R. Kym,† James T. Link,† Hwan-Soo Jae,† Chunqiu Lai,† Theresa Apelqvist,§ Patrik Rhonnstad,§ Lars Hagberg,§ Konrad Koehler,§ Marlena Grynfarb,§ Annika Goos-Nilsson,§ Johnny Sandberg,§ Marie Österlund,§ Tomas Barkhem,§ Marie Höglund,§ Jiahong Wang,† Steven Fung,† Denise Wilcox,† Phong Nguyen,† Clarissa Jakob,‡ Charles Hutchins,‡ Mathias Färnegårdh,§ Björn Kauppi,§ Lars Öhman,§ and Peer B. Jacobson†

Metabolic Disease Research and Structural Biology Departments, Global Pharmaceutical Discovery, Abbott Laboratories, Abbott Park, Illinois 60064, and KaroBio AB, Huddinge, Sweden

Received January 8, 2004

Hepatic blockade of glucocorticoid receptors (GR) suppresses glucose production and thus decreases circulating glucose levels, but systemic glucocorticoid antagonism can produce adrenal insufficiency and other undesirable side effects. These hepatic and systemic responses might be dissected, leading to liver-selective pharmacology, when a GR antagonist is linked to a bile acid in an appropriate manner. Bile acid conjugation can be accomplished with a minimal loss of binding affinity for GR. The resultant conjugates remain potent in cell-based functional assays. A novel in vivo assay has been developed to simultaneously evaluate both hepatic and systemic GR blockade; this assay has been used to optimize the nature and site of the linker functionality, as well as the choice of the GR antagonist and the bile acid. This optimization led to the identification of A-348441, which reduces glucose levels and improves lipid profiles in an animal model of diabetes.

Introduction

Glycemic control depends on a precise match between glucose inputs and outputs; any disturbance in this balance can result in hypo- or hyperglycemia. Glucose is taken in as dietary carbohydrate or is produced in the liver (hepatic glucose output (HGO)); it is consumed in tissues as a primary energy source. Following meals, a glucose-driven increase in circulating insulin levels leads to a stimulation of glucose disposal (primarily in skeletal muscle) and a reduction of HGO. Through the combination of these insulin effects, blood glucose levels show only a small and transient increase after meals. In the fasting state, HGO serves as the primary source of glucose and thus is critical for survival. These responses are tightly regulated; any drop in glucose levels triggers a counter-regulatory hormonal response that will increase hepatic glucose output and restore normoglycemia.

These counter-regulatory responses are out of balance in patients with Type 2 diabetes mellitus (T2DM). Diabetics fail to move glucose into tissues efficiently as circulating levels rise, and these elevated circulating glucose levels fail to appropriately suppress hepatic glucose production. Each of these factors contributes to the hyperglycemia that is the hallmark of this disease. Thus, it is expected that an agent that restores peripheral insulin sensitivity, or decreases HGO, would find use in the treatment of T2DM. There is evidence to suggest that this is indeed the case. Thiazolidinediones such as rosiglitazone (Avandia) or pioglitazone (Actos) improve glycemic status by increasing the insulin response in peripheral tissues, while the antidiabetic properties of metformin (Glucophage) are derived at least in part through a reduction of hepatic glucose production.

Hepatically derived glucose plays a key role in maintaining circulating glucose levels, especially in the fasting state. Changes in the activity of individual enzymes in this pathway can have dramatic metabolic consequences. For example, loss-of-function mutations in key gluconeogenic enzymes (e.g. glucose-6-phosphatase, G6Pase, or fructose-1,6-bisphosphatase, FBPase) trigger human genetic diseases characterized by a dramatic reduction in HGO and resulting episodes of hypoglycemia.[1,2] Conversely, the overexpression of phosphoenolpyruvate carboxykinase (PEPCK) in the liver of transgenic mice is sufficient to produce hyperglycemia and results in an overall phenotype that closely resembles human type 2 diabetes.[3]

The Role of Glucocorticoids. While glucocorticoids have antiinflammatory properties and produce multiple effects on protein, carbohydrate, lipid, and nucleic acid metabolism, they are named in recognition of their primary role in modulating glucose metabolism. Glucocorticoids raise blood glucose levels by functionally antagonizing the action of insulin, thereby inhibiting glucose disposal and promoting hepatic glucose production. The change in HGO is primarily driven by an increase in gluconeogenesis, a result of increased mobilization of gluconeogenic precursors, direct transcriptional stimulation of gluconeogenic enzymes (e.g. PEP-

* Address correspondence to D-47H, AP10-208, Abbott Laboratories, 100 Abbott Park Rd., Abbott Park, IL 60064-6100. E-mail: thomas.vongeldern@abbott.com.
† Metabolic Disease Research, Abbott Laboratories.
‡ Structural Biology, Abbott Laboratories.
§ KaroBio AB.
‖ Current address: S*BIO, 1 Science Park Rd., Singapore.

10.1021/jm0400045 CCC: $27.50
Published on Web 07/13/2004

CK and G6Pase), and interference with insulin signal transduction in the liver.[4] The potent effects of glucocorticoids on glucose metabolism can be observed in human diseases characterized by increased or decreased cortisol production. Patients with an excess of cortisol production (Cushing's disease) have a cluster of symptoms that include impaired glucose tolerance due to insulin resistance and increased gluconeogenesis.[5,6] Overt diabetes occurs in approximately 20% of these patients. On the other hand, a deficit of cortisol production (Addison's disease) results in decreased HGO and occasionally to hypoglycemia.[7] It is worth noting that these changes in cortisol levels modulate global glucose metabolism even when the secretion and action of other hormones involved in glucose homeostasis is unimpaired.

Glucocorticoid receptor (GR) antagonism has been validated as a strategy for regulating HGO in vitro, in animal disease models, and in man. Most of these validation studies have been performed using the prototype GR antagonist mifepristone (RU-486, **1**). Thus, acute treatment of genetically obese and diabetic db/db mice (which lack the satiety hormone leptin) reduces circulating glucose levels by half and normalizes hepatic levels of G6Pase and PEPCK.[3] Longer-term treatment of obese diabetic ob/ob mice (which lack leptin receptor) normalizes postprandial glucose levels and improves insulin sensitivity.[8] Glucose metabolism improves in Cushing's patients who receive mifepristone treatment, as indicated by a 40% reduction in HbA1c levels.[6] And a single dose of a GR antagonist can reduce HGO and fasting glucose levels in normal subjects.[9]

However, long-term systemic GR antagonism may not be a viable approach for the treatment of type 2 diabetes. Experience with extended (up to 12 months) mifepristone treatment suggests that generalized GR antagonism can lead to symptoms of adrenal insufficiency (nausea, vomiting, exhaustion). It is also expected that systemic receptor blockade will be problematic in situations where increased cortisol levels are an advantageous physiologic adaptation to stress,[10] and because peripheral glucococorticoid responsiveness is closely monitored by the hypothalamus, generalized receptor antagonism results in the activation of the hypothalamic−pituitary−adrenal (HPA) axis, causing stimulation of the adrenal cortex (adrenal hyperplasia) and increased cortisol secretion. Neither of these competing outcomes (adrenal insufficiency, hypercortisolemia) is desirable from a patient perspective.

In contrast, a liver-specific derivative of mifepristone would be expected to decrease HGO and improve glucose metabolism without the risk of these peripherally driven side effects. The above considerations have led us to propose liver-selective glucocorticoid antagonism as a novel approach to the treatment of T2DM. Compounds with the target profile would retain the beneficial effects of glucocorticoid blockade to suppress hepatic glucose production; but would avoid the complications associated with the loss of peripheral glucocorticoid response.

Liver Targeting. An extensive literature describes the efforts of researchers to "target" drugs to the liver. Leeson and co-workers report that certain substructural features lead to a reduction in cardiac vs. hepatic activity in a family of thyromimetic T_3 derivatives.[11]

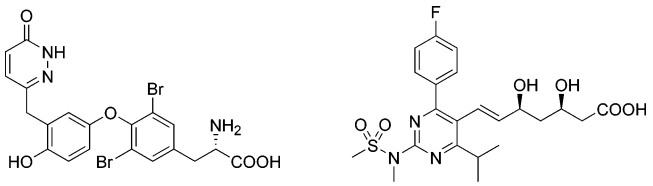

Figure 1. Some compounds reported to exhibit in vivo liver selectivity.

Rosuvastatin has been reported to be unique among HMG-CoA reductase inhibitors in demonstrating liver-selective pharmacology.[12] While it is apparent that specific structural features of these molecules are related to their "intrinsic targeting" properties (Figure 1), the structure−function correlations do not provide a clear strategy to identify liver-selective variants of other drugs.

Efforts to rationally develop generic liver targeting strategies have generally employed an "address-and-message" approach. The bioactive agent in question is attached ("conjugated") to a vector intended to direct distribution selectively to the liver. As a rule, these vectors are selected based on their high affinity for specific hepatic structures; sialo- and asialoglycoproteins[13,14] and neoglyco- and neopeptide albumins[15] have all been studied as targeting agents. Liposomes have been galactosylated to select for their uptake into hepatocytes.[16] Triglyceride hydrolysis has been used as a means to release active drug in the liver.[17] Except in the latter case, these conjugates can only be administered through intravenous injection.

In principle, bile acids offer a unique solution to the problem of liver targeting which is compatible with oral delivery of a therapeutic agent. Naturally occurring bile acids are tightly constrained within the enterohepatic loop through the action of a series of transporter proteins.[18] These highly efficient enteric and hepatic uptake mechanisms ensure that less than 2% of the total bile acid pool is excreted daily, even as it makes 10 or more passes through the intestine, portal vein, liver, and bile duct. A bile acid conjugate that retained these properties would be expected to have exceptionally high bioavailability as well as substantial hepatic levels and a high liver-to-plasma (or -tissue) ratio.

A number of researchers have attempted to probe this mechanism for hepatic targeting.[19−23] Of particular note is the work of Kramer and co-workers at Aventis. These workers have attached bile acids to dye molecules (allowing them to track distribution), to small peptide fragments, and to oligonucleotides (Figure 2). They have demonstrated in a series of elegant experiments that these conjugate molecules are recognized by bile acid transport systems,[19,20] and that they are trafficked through the liver in a manner similar to a bile acid.[21,22] But none of these conjugates has been shown to deliver intact conjugate when dosed orally. In fact, Borchardt and co-workers have questioned the role of transporters in moving molecules of this type, noting that while bile acid−peptide conjugates can bind to transporters, they are not themselves transported.[23] Thus, several key questions regarding the value of bile acid transport as a means to deliver oral pharmaceuticals selectively to the liver remain unanswered. The primary goal of the

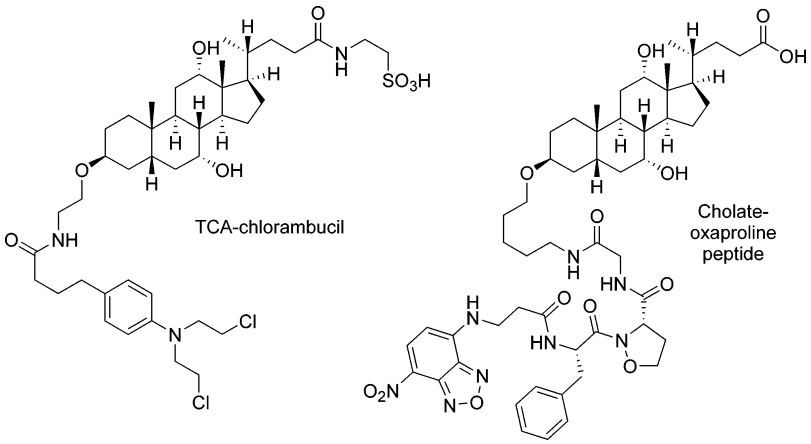

Figure 2. Bile acid conjugation has been employed to alter the distribution of a number of pharmacologic agents, including chlorambucil and an inhibitor of prolyl-4-hydroxylase (**22**).

Scheme 1. Derivatization of Mifepristone. Compound **2** Is a Key Intermediate in the Preparation of Bile Acid-Conjugated Mifepristone Derivatives[a]

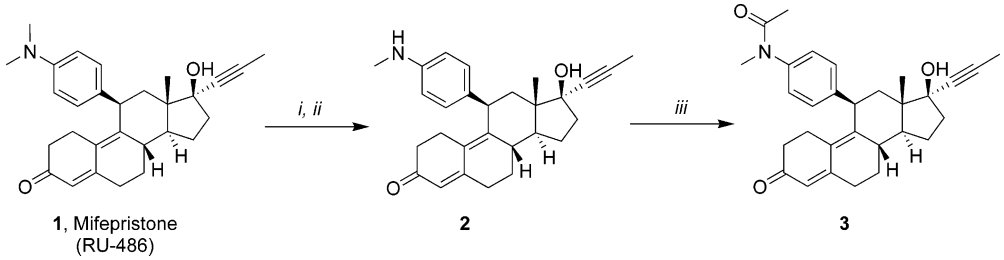

[a] Reagents and conditions: *i*. TPAP, NMO, CH_2Cl_2; *ii*. aq HCl, MeOH; *iii*. Ac_2O, pyr, 60 °C.

Scheme 2. C17-Linked Conjugate **15** Is Prepared from **2** through a Sequence of Acylations[a]

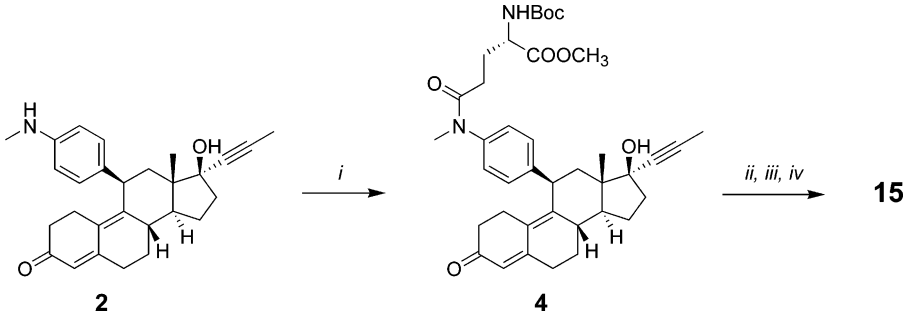

[a] Reagents and conditions: *i*. Boc-Glu-OMe, TBTU, *i*-Pr_2NEt, DMF; *ii*. HCl/EtOAc; *iii*. cholic acid, TBTU, *i*-Pr_2NEt, DMF; *iv*. LiOH, H_2O-THF.

present study was to address these questions in the context of preparing a liver-targeted derivative of mifepristone (**1**).

Chemistry. In general, the bile acid conjugates described herein are assembled from two primary fragments, derived respectively from a glucocorticoid antagonist and a naturally occurring bile acid. GR antagonist fragment **2** was initially prepared from commercially available **1** using the radical dealkylation procedure of Acosta et al.[24] In our hands this procedure gave variable results and was particularly problematic when scaled up. For this reason we have developed a new procedure[25] for dealkylating this *N*,*N*-dimethylaniline (Scheme 1). Treatment of **1** with TPAP cleanly oxidizes one methyl group to give an *N*-formyl derivative, which can be hydrolyzed under mildly acidic conditions to provide **2** in 60% overall yield. Bile acid derivatives are generally prepared from cholic acid as a starting material. The glycocholate derivative **4** is prepared by coupling the acid with a suitably protected glutamate analogue, followed by selective removal of the side chain protecting group (Scheme 2). Other derivatives (see Scheme 3) take advantage of the known reactivity order of the three hydroxyl groups, C3−OH > C7−OH > C12−OH. For example, the C3−OH may be selectively acylated to give intermediates such as **5** and **6**, or selectively activated via sulfonylation and displaced with a diol, as originally reported by Kramer and co-workers,[19] to give the inverted ether **7** (after activation of the remaining primary alcohol). Protection of the C3-alcohol, via formation of the mono-acetate, allows for acylation at C7 to provide derivatives such as **10** and **12**. When the C7-OH is also protected, for example by formation of the 3,7-diacetate, reaction occurs at the hindered C12 site to give intermediates such as **13**. The formation of C3α ether-linked intermediate **8**, retaining the natural

Scheme 3. Synthesis of Bile Acid-Based Intermediates[a]

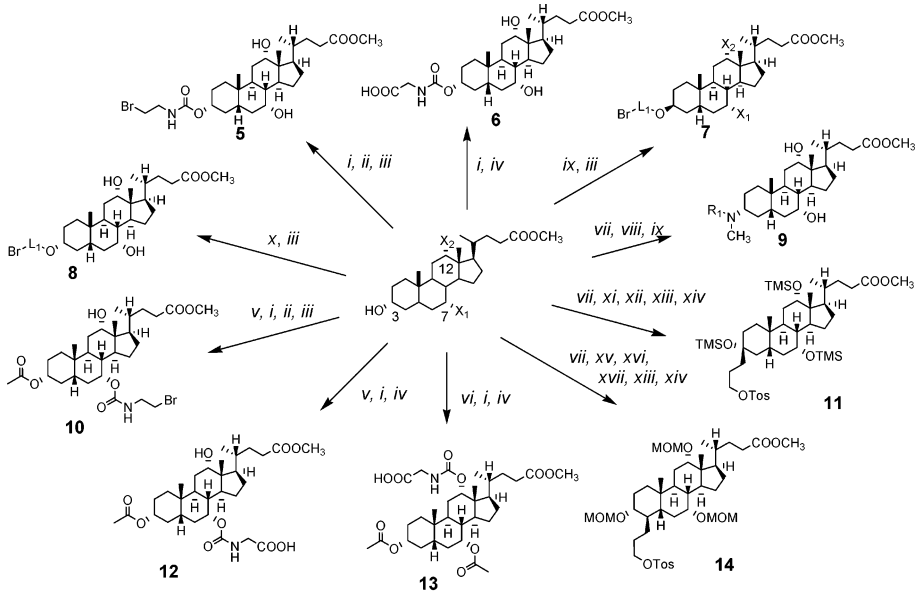

X_1, X_2 = H,OH ; L_1 = $-(CH_2)_2-$, $-(CH_2)_3-$, $-(CH_2)_2O(CH_2)_2-$; R_1 = $Br(CH_2)_3CO-$, $Br(CH_2)_2NHCO-$, $Br(CH_2)_3SO_2-$

[a] Reagents and conditions: *i*. *p*-NP-OCOCl, pyr, 60 °C; *ii*. 2-aminoethanol, NMM, dioxane/water, 50 °C; *iii*. NBS, PPh_3, DMF; glycine, NMM, dioxane/water, 50 °C; *iv*. glycine, NMM, dioxane/water, 50 °C; *v*. Ac_2O (1.1 equiv), DMAP, pyr; *vi*. Ac_2O (2.2 equiv), DMAP, pyr; *vii*. Ag_2CO_3, Celite, tol, reflux/$-H_2O$; *viii*. CH_3NH_2, $NaCNBH_3$, AcOH, MeOH/CH_3CN; *ix*. R1-Cl, *i*-Pr_2NEt, CH_3CN; *x*. ref. 19; *xi*. Zn, allyl iodide, THF; *xii*. TMS-Cl, imidazole, DMF; *xiii*. 9-BBN, THF; Me_3NO, 60 °C; *xiv*. TsCl, pyr; xv. MOM-Cl, *i*-Pr_2NEt, DCE, 45 °C; xvi. allyl bromide, KOtBu, THF, 0 °C; *xvii*. $NaBH_4$, MeOH.

configuration of the bile acid, is also possible, but ironically this alkylation is most successful when the C7- and C12-hydroxyls are protected as acetates.[19]

The C3-OH can also be selectively oxidized, using Tserng's modification of the Fetizon oxidation.[26] The resultant ketone can be used as the substrate for a reductive amination, which in the case of methylamine provides the α-epimer **9** as the major product (>5:1). Alternatively, the enolate can be alkylated with allyl bromide (alkylation occurs with high selectivity on the *β*-face of C4); or the ketone can be reacted with an allylzinc reagent (approach of the nucleophile again occurs from the *β*-face, reestablishing the α-alcohol stereochemistry). In each of these latter cases, further elaboration of the allyl group provides the coupling intermediate (**14** and **11**, respectively).

Coupling of GR antagonist and bile acid-based fragments is accomplished in straightforward fashion (Scheme 4). Anilide-based conjugates such as **15**, **16a**, **19a**, and **20** are formed by in situ activation of the acid fragment under standard amide bond-forming conditions (generally EDCI/HOBt or TBTU). Aniline-based couplings (i.e. to give **16b**−**k**, **17**, **18**, and **19b**) are accomplished by warming an acetonitrile solution of the coupling partners in the presence of an amine base. When the electrophile is a sulfonate ester, the addition of an iodide source to the reaction mixture catalyzes the process; alternatively the alkyl iodide may be preformed and used directly in the reaction. Hydrolysis of the ester functionality under alkaline conditions completes the synthesis of the bile acid conjugates.

Other bile acids can provide the basis for the address component of these conjugate molecules. Thus, for example, deoxycholic acid, chenodeoxycholic acid, and lithocholic acid can be subjected to the synthetic procedures described above to produce the corresponding derivatives. Conjugates based on glycocholic or taurocholic acids are prepared through an alternative strategy that involves assembly of the intact cholate conjugate **16c***β*, followed by coupling with glycine or taurine to generate the final product (Scheme 5).

Compound Evaluation. All compounds are evaluated for their ability to bind to the glucocorticoid receptor, employing a standard radioligand binding assay and using [^{3}H]-dexamethasone, a potent agonist, as the reference radioligand. A similar format is used to measure the affinity of selected compounds for other steroid hormone receptors. A typical "receptogram" includes androgen (AR), estrogen (ERα and ER*β*), mineralocorticoid (MR), progesterone (PR), and thyroid hormone (TRα and TR*β*) receptors.

Functional activity is evaluated using two distinct cell-based assay systems. GRAF (in Swedish, "**GR** linked to **A**lkaline **F**osfatase") cells are a genetically engineered mammalian cell line expressing GR. Based on a Chinese hamster ovarian (CHO) cell line, GRAF cells also contain a stably integrated artificial transcription unit composed of a glucocorticoid hormone response element (GRE) and core promoter sequences fused to a downstream reporter gene encoding a secreted form of alkaline phosphatase (ALP). Compounds are evaluated for antagonism of dexamethasone-induced ALP expression. GRAF cells can also be used to determine intrinsic agonist activity of analogues. Compounds may also be evaluated for activity in hepatocytes, the intended target cell. Primary rat hepatocytes are stimulated with dexamethasone ("dex"), leading to the increase in expression in a number of GR-regulated proteins. The enzyme tyrosine aminotransferase (TAT) is chosen as a marker for GR activation. TAT is known to be regulated by hepatic glucocorticoid, but is not directly on the pathway leading to increased hepatic glucose production. It is

Scheme 4. Bile Acid Conjugates Are Assembled from Intermediate Fragments via Acylation or Alkylation Strategies

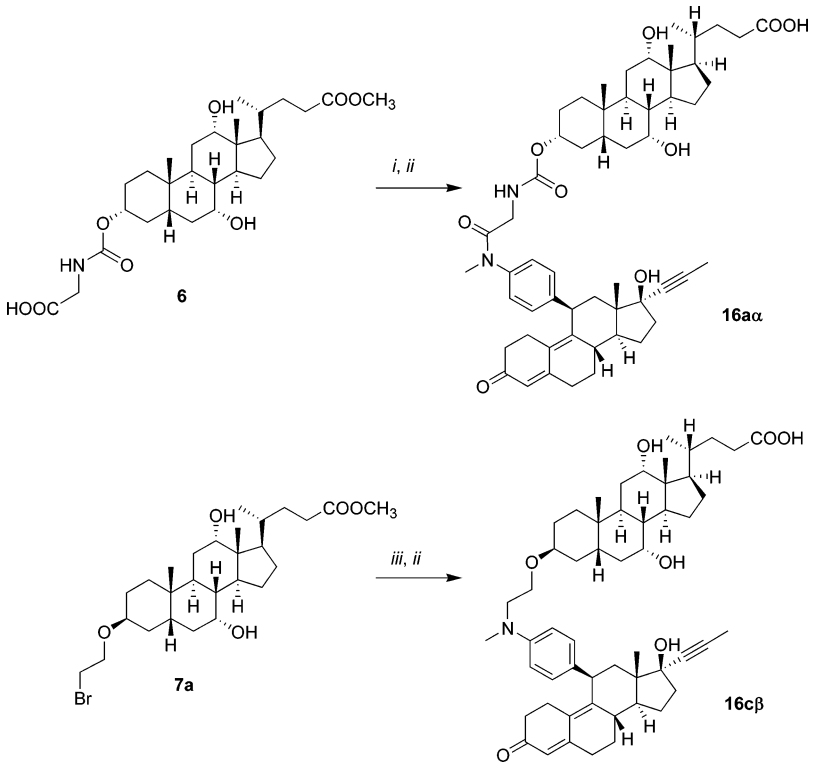

[a] Reagents and conditions: *i*. compound **2**, TBTU, DMF; *ii*. LiOH, H_2O/THF; *iii*. compound **2**, *i*-Pr_2NEt, NaI, CH_3CN, 100 °C

Scheme 5. Glycocholate and Taurocholate Conjugates **21a** and **21b** Are Prepared by Coupling **16c**β with Glycine and Taurine, Respectively

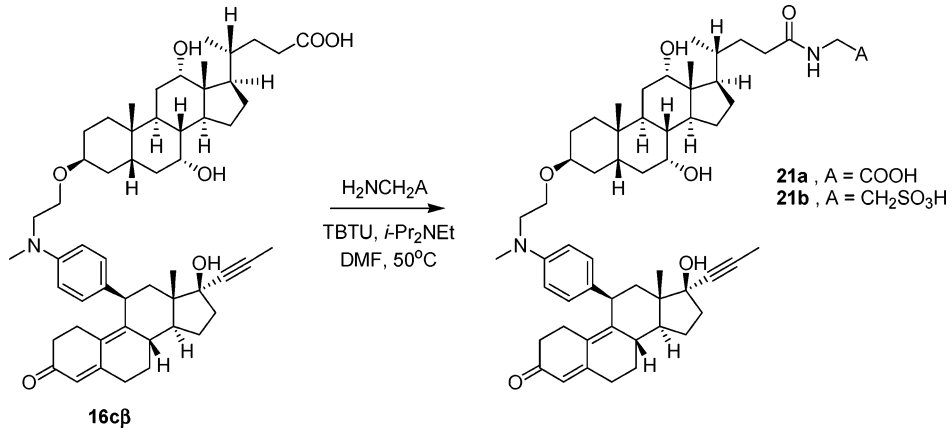

selected for practical reasons; dex increases TAT levels 2−3-fold over the course of a 4-h incubation, a far greater window than is observed with key gluconeogenic enzymes such as PEPCK or G6Pase.

The use of surrogate markers of glucocorticoid activation also provides a basis for the in vivo evaluation of efficacy and liver selectivity. In a rat prednisolone challenge (RPC) experiment, normal fasted Sprague−Dawley rats are given an oral dose of prednisolone, another glucocorticoid agonist. Prednisolone (pred) is systemically available and produces GR-mediated responses in peripheral tissues as well as in the liver. In particular, it increases hepatic levels of TAT, stimulates the deposition of glycogen in the liver, and blocks the production of circulating lymphocytes (part of the basis for its antiinflammatory effect). A systemic glucocorticoid antagonist like **1**, given prior to the pred challenge, will block not only the increases in TAT and glycogen levels but also the lymphopenic response. A liver-selective agent would modulate TAT and glycogen responses but have no effect on lymphocyte levels.

Results and Discussion

For the "address-and-message" strategy embodied in the production of conjugate molecules such as **15**−**21** to be successful, each component of the conjugate must retain most, if not all, of its desirable characteristics. Thus, for example, compounds **15**−**21** must bind tightly to the glucocorticoid receptor, despite the attachment of a large bile acid moiety. Similarly, the bile acid fragment of **15**−**21** must be capable of directing liver-selective distribution and/or pharmacology, even while it is attached to a large GR antagonist unit. It is clear that the details of the attachment of these two functionalities, as well as the nature of the linking unit itself, will play a critical role in defining the properties

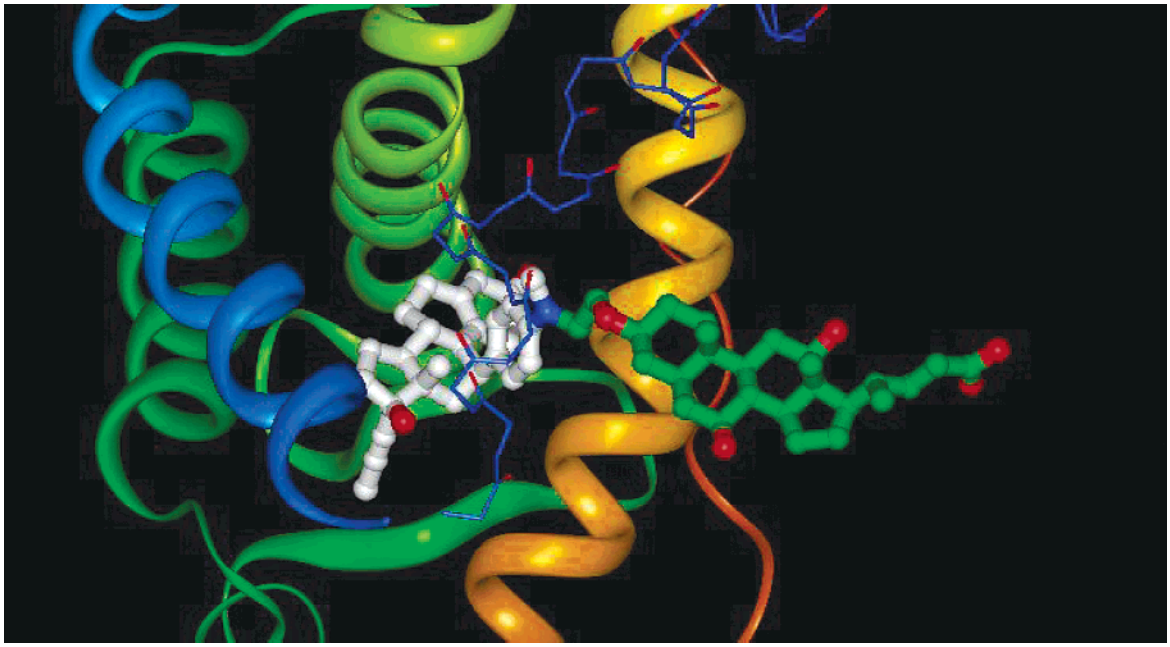

Figure 3. Computer model of **16c**β bound to the GR ligand-binding domain (GR-LBD). Model is based on the X-ray crystal structure of mifepristone (**1**)/GR-LBD complex.[27]

of the conjugates. Initial structure−activity studies probed this question in some detail. We began with the question of how to attach a bile acid fragment to a glucocorticoid antagonist while retaining GR affinity. The X-ray crystal structure of the GR ligand-binding domain (GR-LBD) recently reported by our group,[27] and including mifepristone as ligand, provided valuable assistance in addressing this issue. The major structural features of GR-LBD are consistent with those reported for other nuclear hormone receptors such as PR,[28] defined by an antiparallel sandwich of α-helical layers. The ligand sits within a large hydrophobic binding cavity, with key hydrogen-bonding contacts involving the C3-ketone (to Gln-570 and Arg-611) and C17β-hydroxyl (to Gln-642 and to a tightly bound water molecule held in place by Cys-736). The *p*-dimethylamino group on the C-11 aromatic ring protrudes from this binding pocket, accessing solvent-exposed space. By analogy with earlier studies on PR,[28] it is this group which displaces helix 12 from its characteristic agonist position sitting over (and capping) the binding cavity; this forces the receptor/ligand complex into an antagonist conformation. The solvent-accessibility of this amine also suggests it as a logical site for attachment of a large molecular fragment, such as a bile acid (see model in Figure 3, based on X-ray structure of mifepristone/GR-LBD complex). In practice, we have explored two chemical strategies for linking through the C-11 aniline. Compounds such as **15**, **16a**, **19a**, and **20**, which are coupled through an activated acid to give an anilide-containing linker, generally exhibit GR affinities between 1 and 7 nM (K_I) range, with an average for this subclass of 2.3 nM (data summarized in Table 1). While these analogues are active, supporting the premise that the C-11 substituent can tolerate a large modification, they are nonetheless substantially less potent than the parent **1** ($K_I = 0.1$ nM). These conjugate molecules have two features that distinguish them from the parent: a large bile acid substituent has been attached, and the nature of the aniline group has been altered by the presence of the amide group. How much of the change in binding affinity is due to each of these modifications? A comparison of **1** with the corresponding *N*-acetyl analogue **3** ($IC_{50} = 0.4$ nM) suggests that the *N*-acyl linkage contributes substantially to the observed loss of potency. To test this hypothesis, a series of *N*-alkyl-modified analogues (**16b**−**k**, **17**, **18**, **19b**) have been prepared by alkylation of the methylaniline **2**. These compounds recover the ∼4-fold loss of activity due to the presence of the amide; they exhibit GR affinities in the 0.11−1 nM range, with a mean K_I of 0.33 nM for this group. When properly linked, the cost (in GR binding affinity) of attaching a bile acid substituent can be 3-fold or less.

Conjugation with the bile acid also has relatively little effect on the affinity of these analogues for other nuclear hormone receptors (Table 1). In addition to its role as a GR antagonist, mifepristone has potent interactions with both the progestin ($K_I = 0.64$ nM) and androgen ($K_I = 0.65$ nM) receptors. Acylation of the C-11 aniline nitrogen, as in **3**, **15**, **16a**, **19a**, or **20**, reduces PR binding affinity as was observed in the GR binding assay. Most importantly, there seems to be no particular advantage (nor disadvantage) in terms of GR:PR selectivity to adding the bile acid moiety to these GR antagonists. Similar results are observed with ER, MR, and TR, against which selectivity is generally quite high. The exception to these trends comes in the case of androgen receptor. The modest selectivity of mifepristone for GR over AR (6-fold) improves significantly upon conjugation. Conjugates have GR:AR ratios which vary from 10 to 70, averaging 25-fold. No obvious SAR trends emerge.

The role of the bile acid moiety is examined obliquely, by determining the potency of analogues in several functional assays in intact cells. GRAF cells, which do not contain bile acid transporters, are expected to provide some indication of the ability of the various conjugates to penetrate cells passively. A comparison

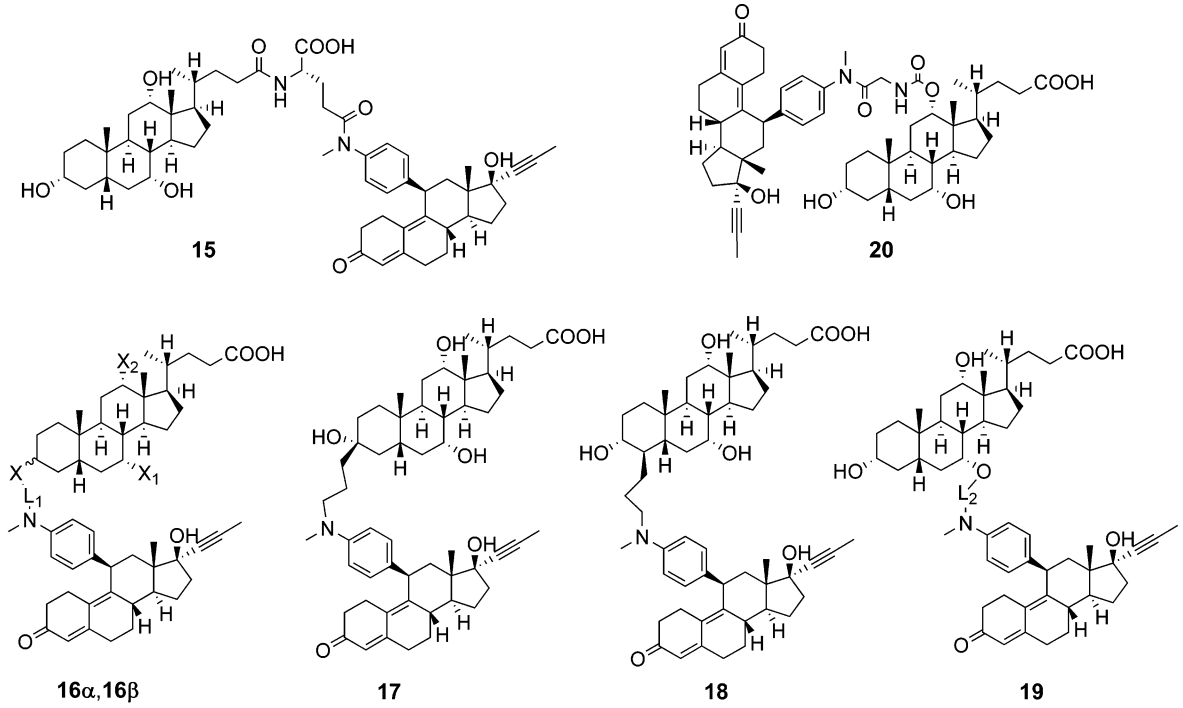

$X_1 = X_2 = OH$
- **a.** XL_1 = -OC(O)NHCH$_2$C(O)-
- **b.** XL_1 = -OC(O)NH(CH$_2$)$_2$-
- **c.** XL_1 = -O(CH$_2$)$_2$-
- **d.** XL_1 = -N(Me)C(O)(CH$_2$)$_3$-
- **e.** XL_1 = -N(Me)C(O)NH(CH$_2$)$_2$-
- **f.** XL_1 = -N(Me)S(O)$_2$(CH$_2$)$_3$-
- **g.** XL_1 = -O(CH$_2$)$_3$-
- **h.** XL_1 = -O(CH$_2$)$_2$O(CH$_2$)$_2$-

XL_1 = -O(CH$_2$)$_2$-
- **i.** X_1 = H, X_2 = OH
- **j.** X_1 = OH, X_2 = H
- **k.** $X_1 = X_2$ = H

a. L_2 = -C(O)NHCH$_2$C(O)-
b. L_2 = -C(O)NH(CH$_2$)$_2$-

Figure 4. Bile acid-conjugated glucocorticoid receptor antagonists.

of mifepristone, the acetamide **3**, and the conjugated analogues produces the following conclusions:

1. All of the compounds prepared for this study are full functional antagonists in this assay, with minimal agonist activity. The maximal blockade of dexamethasone-induced alkaline phosphatase production produced by the conjugates varies from 75 to 100%, and averages >90%.

2. None of the conjugates is superior to the parent **1** in the GRAF assay. Most analogues are 3−50 times less potent than **1**.

3. Analogues **21a** and **21b**, based on the "conjugated" bile acids glycocholate and taurocholate, are relatively poor antagonists in the GRAF assay; K_I values are 7- and 30-fold higher than the parent **16c**β. This loss of activity may be due to decreased cell permeability; **21b** exhibits a very low flux rate in caco-2 cells (Papp $< 5 \times 10^{-8}$ cm/s, unpublished results).

4. Following the trend previously observed in the GR binding assay, anilides are less active than the corresponding anilines; the mean K_I for **15**, **16a**, **19a**, and **20** is 88 nM, vs 4.4 nM for the remainder of the analogues. In the single instance where a direct comparison is possible, **16b**α is $\sim$35$\times$ more potent than **16a**α.

5. The data set is not complete enough to allow a clear evaluation of the role of the linkage site on GRAF activity. C3-linked conjugates tend to be more potent than those linked at other positions on the bile acid fragment; the mean K_I for the C3-linked compounds is 3.7 nM, while the average for those linked at other sites (**15**, **18**, **19**, and **20**) is 75 nM. This result is strongly biased by the fact that all non-C3-linked conjugates are anilides; which have been demonstrated to be less potent in the GRAF assay (point 3 above). When this confounding factor is removed, the trends are less apparent. The C3-amide-linked **16a**α is no different in activity than C7- and C12- variants (**19a** and **20**, respectively); on the other hand, the C4-aniline **18** (52 nM) is far less active than a typical C3-aniline (average $K_I = 3.1$ nM).

6. It *is* clear that, within the C3-linked analogues, conjugates linked on the β-face of the bile acid are superior to those linked on the α-face. The average

Table 1. In Vitro Activity of GR Antagonist Molecules

compd	GR[a]	PR[a]	MR[a]	AR[a]	ERα[a]	ERβ[a]	TRα[a]	TRβ[a]	GRAF[a]	HepTAT[a]
1	0.10 (0.09−0.11, 2)	0.64 (1)	640 (1)	0.65 (1)	>200 (1)	>750 (1)	>1,250 (1)	>2250 (1)	0.44 (0.4−0.46, 2)	120 (39−180, 8)
3	0.4 (0.24−0.66, 2)	6.4 (1)	>1000 (1)	8.9 (1)	34 (1)	570 (1)	790 (1)	>2250 (1)	1.4 (1.1−1.6, 2)	ND
15	3.0 (1.0−6.3, 8)	1.2 (1)	590 (1)	34 (1)	72 (1)	240 (1)	1200 (1)	>2250 (1)	250 (190−310, 3)	350 (200−610, 2)
16aα	2.1 (1.8−2.8, 4)	2.4 (2.4−2.5, 2)	310 (210−460, 2)	21 (1)	11 (1)	160 (1)	1100 (1)	>2250 (1)	50 (26−99, 2)	340 (170−540, 3)
16bα	0.39 (0.35−0.43, 2)	0.39 (1)	>1000 (1)	6.2 (1)	>200 (1)	>750 (1)	>1250 (1)	>2250 (1)	1.4 (1)	330 (330−340, 2)
16cα	0.67 (0.3−1.4, 4)	3.3 (0.79−14, 2)	>1000 (1)	8.9 (6.3−12, 2)	11 (7.4−15, 2)	89 (47−170, 2)	>1250 (1)	>2250 (1)	11 (2.7−73, 4)	220 (150−390, 3)
16cβ	0.27 (0.1−1.5, 20)	0.81 (0.18−2.8, 15)	440 (220−1800, 8)	8.1 (4.4−29, 8)	12 (9−74, 7)	110 (1)	670 (340−1700, 7)	1500 (900−5400, 7)	1.1 (0.45−2.3, 9)	56 (34−100, 10)
16dα	0.27 (0.16−0.46, 2)	0.96 (1)	190 (1)	7.4 (1)	6.2 (1)	13 (1)	>1250 (1)	>2250 (1)	1.2 (1)	60 (47−81, 2)
16eα	0.30 (0.27−0.33, 2)	3.5 (1)	850 (1)	16 (1)	140 (1)	190 (1)	>1250 (1)	>2250 (1)	15 (1)	34 (21−60, 2)
16fα	0.42 (0.32−0.61, 4)	1.9 (1)	300 (270−350, 2)	17 (13−22, 2)	19 (14−28, 2)	39 (24−63, 2)	ND	ND	15 (14−16, 2)	60 (56−64, 2)
16gβ	0.22 (0.18−0.26, 2)	1.1 (1)	80 (1)	4.6 (1)	8.8 (1)	13 (1)	>1250 (1)	1900 (1)	1.1 (1)	100 (81−130, 2)
16hα	0.21 (0.20−0.23, 2)	1.7 (1)	170 (1)	4.8 (1)	ND	ND	ND	ND	12 (1)	90 (90−90, 2)
16hβ	0.17 (0.11−0.27, 6)	0.48 (0.39−0.64, 3)	150 (1)	3.3 (1)	14 (1)	51 (1)	>1250 (1)	>2250 (1)	1.1 (1.0−1.3, 3)	56 (51−60, 2)
16iβ	0.16 (0.14−0.19, 2)	ND	ND	ND	ND	ND	ND	ND	0.38 (1)	ND
16jβ	0.18 (0.17−0.20, 2)	ND	ND	ND	ND	ND	ND	ND	0.76 (1)	ND
16kβ	0.22 (0.20−0.25, 2)	ND	ND	ND	ND	ND	ND	ND	2.7 (1)	ND
17β	0.11 (0.06−0.16, 3)	ND	ND	ND	ND	ND	ND	ND	4.3 (4.0−4.6, 2)	ND
18β	0.80 (0.7−0.9, 2)	2.1 (1.9−2.2, 2)	>1000 (1)	53 (1)	46 (1)	48 (1)	ND	ND	52 (1)	340 (300−380, 2)
19aα	1.1 (1.1−1.2, 2)	4.4 (1)	>1000 (1)	37 (1)	94 (1)	>750 (1)	>1250 (1)	>2250 (1)	49 (1)	230 (150−330, 2)
19bα	1.2 (0.87−1.7, 3)	4.6 (1)	310 (1)	18 (1)	ND	ND	ND	ND	37 (1)	730 (360−1300, 5)
20α	6.5 (4.8−8.2, 3)	ND	ND	ND	ND	ND	ND	ND	100 (1)	500 (460−550, 2)
21aβ	0.42 (0.42−0.43, 2)	1.0 (1)	510 (1)	34 (1)	ND	ND	>1250 (1)	>2250 (1)	8.6 (1)	180 (150−300, 3)
21bβ	0.27 (0.17−0.38, 4)	0.53 (1)	140 (1)	8.9 (1)	10 (1)	30 (1)	>1250 (1)	>2250 (1)	37 (1.9−67, 2)	160 (130−220, 4)

[a] All K_I values reported in nM, as geometric mean, (range, *N*). Each $N = 1$ refers to the average of two experiments performed on the same sample; each experimental value is measured in duplicate.

GRAF K_I for the α-linked analogues is 11 nM; while the β-linked conjugates average 1.2 nM. In the two cases where a direct comparison is possible, both **16c**β and **16h**β (each 1.1 nM) are 10× more potent than their α-linked comparators **16c**α and **16h**α (11 nM and 12 nM). This paradoxical observation, that the more active conjugate series is attached on the face *opposite* that of a native bile acid, cannot readily be explained on the basis of physicochemical properties such as logD or polar surface area (PSA). It is, however, consistent with previous reports by Kramer and co-workers.[20−22]

7. A variety of bile acids are tolerated. While most of the analogues shown are built from cholic acid, the predominant native bile acid, the GRAF activity of conjugates incorporating deoxycholic (**16i**β, 0.38 nM), chenodeoxycholic (**16j**β, 0.76 nM), and lithocholic (**16k**β, 2.7 nM) have similar activity to the cholate comparator **16c**β (1.1 nM).

The hepatocyte TAT assay provides a cellular readout that factors in several additional parameters. These cells carry functional bile acid importers and exporters, so that intracellular drug concentrations are likely to be regulated through a balance of active and passive uptake and secretion pathways. In addition, primary hepatocytes are metabolically competent, so that metabolism may play a role in determining the availability of active drug within the cells. As a consequence, all of the compounds in this study (including **1**) are less potent in the TAT assay than in GRAF cells, and the differences in activity between compounds is less dramatic (only a 20-fold potency difference between the best and worst compounds). Several structure−activity trends are observed, however:

1. In contrast to the results in the GRAF assay, a number of the bile acid conjugates are superior to mifepristone in hepatocytes. This result may provide indirect evidence that the analogues are actively transported into these cells; alternatively it might represent a change in the metabolic profile of the conjugates. In fact, while we have no direct evidence on the first of these points, we have been able to demonstrate that the conjugates *are* more stable than the parent in hepatocytes. In these experiments (representative results shown in Figure 5) compounds are incubated with primary rat hepatocytes, and the consumption of starting drug is evaluated by HPLC. While mifepristone is converted rapidly under these experimental conditions, the bile acid conjugates (represented here by compound **15**) are essentially unchanged over the course of the incubation.

2. Consistent with the trend in the GRAF assay, conjugates linked at C4, C7, C12, and C21 are inferior

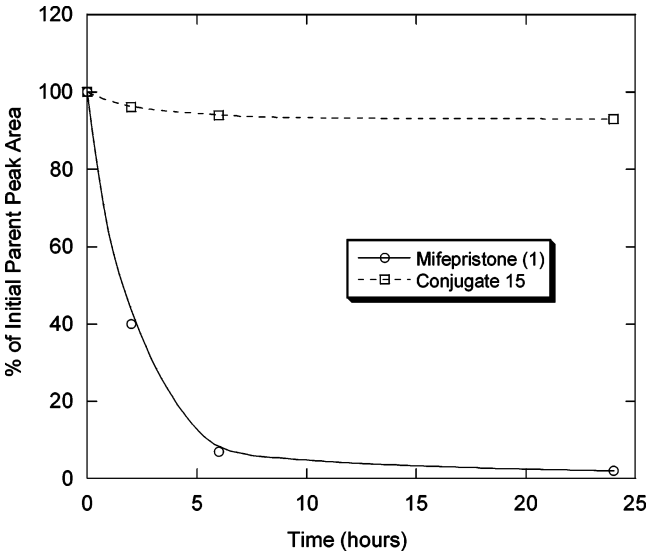

Figure 5. Hepatocyte stability studies of bile acid-conjugated GR antagonist **15**. The bile acid conjugate is substantially protected against metabolism upon incubation with primary rat hepatocytes ($T_{1/2} \gg 24$ h), as compared to parent **1** ($T_{1/2} <$ 2 h).

to C3-linked conjugates. The average K_I for all C3-linked analogues is 110 nM, which is substantially lower than any of the non-C3's.

3. Among the C3-linked analogues, the amine-linked compounds are notably active in the TAT assay. Compounds **16d**α, **16e**α, and **16f**α, which are linked on the α-face through amide, urea, and sulfonamide linkages, comprise three of the top five most active analogues; though it is important to note that many of the differences in potency recorded for the TAT assay in Table 1 are not statistically significant.

4. Of the oxygen-linked conjugates, β-linked conjugates are superior to those linked on the α-face of the bile acid. The mean TAT activity for **16a**α, **16b**α, and **16c**α is 290 nM; for **16c**β, **16g**β, **16h**β, **21a**β, and **21b**β the average is 98 nM. In the one case where a direct comparison is possible, **16c**β (56 nM) is 4-fold more potent than **16a**α (220 nM).

Compounds with superior profiles in the GRAF and hepatocyte assays were next subjected to in vivo evaluation. The rat prednisolone challenge is designed as a primary screening assay to provide a simultaneous look at two key parameters. Hepatic activity is demonstrated by the blockade of pred-stimulated TAT production and through inhibition of pred-induced glycogen deposition. Systemic selectivity is measured by the ability (or inability) of the conjugate molecules to inhibit the antiinflammatory effect of pred, as determined through evaluation of circulating lymphocyte levels. As summarized in Table 2, there is little doubt that our conjugation strategy has succeeded in suppressing the peripheral GR antagonist properties of these compounds. Of the analogues tested, only **16h**β shows any significant ability to block pred-induced lymphopenia, while mifepristone itself completely blocks this response at the test dose of 100 mg/kg.

None of the bile acid conjugates is as active as **1** at inhibiting hepatic glucocorticoid responses. **1** normalizes pred-elevated TAT levels at a 100 mg/kg oral dose and completely suppresses pred-induced increases in glycogen deposition. For each of these hepatic responses, the greatest blockade produced by a conjugate molecule comes from **16c**β, which inhibits TAT by 72% and glycogen levels by 86%. Several structure−activity relationships emerge from this study. Compounds that are attached to the bile acid through a C3-ether linkage (**16c**α, **16c**β, **16g**β, **16h**α, and **16h**β) are clearly superior to those linked via nitrogen (**16d**α, **16f**α) or through a carbamate (**16b**α). The failure of the N-linked analogues, which were among the most potent in hepatocytes, is particularly notable. Among the ether-linked derivatives, there is relatively little difference between linkers of differing lengths (compare **16c**β with **16g**β and **16h**β) or between α- and β-face linked conjugates (**16c**α vs **16c**β; **16h**α vs **16h**β). While the former trend mirrors the in vitro cellular potencies of the analogues, the latter does not.

Table 2. In Vivo Activity of GR Antagonist Molecules

	% inhibition of pred response		
compd	lymphocytes	TAT	glycogen
1	104	101	77
16bα	14	−16	−20
16cα	−14	49	46
16cβ	9	72	86
16dα	4	11	20
16fα	9	−19	9
16gβ	−5	64	43
16hα	−2	66	50
16hβ	43	60	45
16iβ	22	69	38
17β	0	6	5
21b	−6	−63	3
22	−16	5	ND

The data from these rat prednisolone challenge studies support the premise that bile acid conjugation might lead to a functionally liver-targeted glucocorticoid antagonist. Conjugate molecules such as **16c**α, **16c**β, **16g**β, **16h**α, and **16h**β are effective in blunting pred's hepatic effects, while leaving its systemic lymphopenic response intact. Compound **16c**β is particularly effective in this model. To test whether these surrogate markers of glucocorticoid activity accurately capture the compounds' properties, **16c**β has been characterized further in in vivo models that directly assess its antidiabetic activity and its propensity for producing undesirable, peripherally mediated side effects such as HPA activation.

Antidiabetic Efficacy and Side Effect Profiling. The model selected for the evaluation of compound **16c**β (A-348441) as an antidiabetic agent is the ob/ob mouse. These animals, which have a genetic defect blocking the production of the satiety hormone leptin, are obese, hyperphagic, and insulin resistant and thus serve as an excellent model for human Type 2 diabetes. They have been used to characterize a number of commercial antidiabetic and antilipidemic agents including metformin, fenofibrate, and the thiazolidinediones. In the experiment at hand (data shown in Figure 6), the compound is dosed orally, once a day, at 10, 30, and 100 mg/kg, over a period of 6 weeks. Postprandial plasma glucose levels are measured every week, and are compared with normal animals, with untreated ob/ob mice, and with ob/ob mice treated with metformin (500 mg/kg qd). Compound **16c**β clearly lowers plasma glucose levels in a time-dependent and dose-dependent fashion.

a

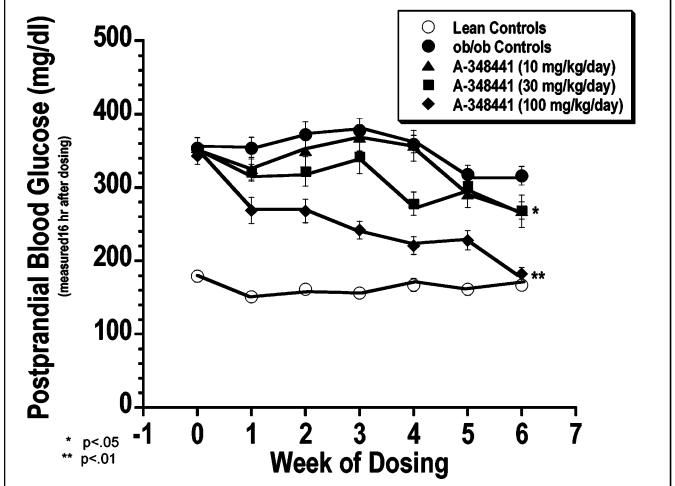

b

Metabolic Parameters

	Lean	*ob/ob* control	A-348441 (100 mpk)
HbA_{1c}	4.3%	10.0%	5.3%
Serum Cholesterol	190 mg/dL (+/-8)	320mg/dL (+/-12)	260 mg/dL (+/-14)
Serum Triglycerides	136 mg/dL (+/-10)	292mg/dL (+/-26)	98 mg/dL (+/-9)
Free Fatty Acids	0.76 mg/dL (+/-0.04)	1.14 mg/dL (+/-0.05)	0.63 mg/dL (+/-0.09)

Figure 6. Chronic effects of A-348441 (**16c**β) in the diabetic *ob/ob* mouse model. Compound is administered orally, qd to ob/ob mice ($N = 8$/group); plasma glucose determinations are made at the start of the study and on a weekly basis. Glucose values are recorded 16 h postdose (a). Measurements of HbA_{1c} and lipid levels are made at beginning and end of study (b).

The onset of the effect is relatively slow, but by the end of the dosing period, glucose levels have actually normalized in the 100 mg/kg group. The lower doses produce smaller responses, which still reach statistical significance by the end of the study. It is important to note that glucose levels are measured 18 h after the once-daily dose; so the effects observed clearly indicate a long-term improvement in glycemic control.

This observation is reinforced by end-of-study measurements of glycated hemoglobin (HbA_{1c}) levels. Glycated protein levels are a good indication of long-term glycemic status and are used as such in clinical practice. An HbA_{1c} change of 1% is considered to be clinically relevant and has been shown to correlate with a substantial improvement in long-term outcomes for a diabetic patient.[29] Ob/ob mice have levels of HbA_{1c} (typically 8−10%) that are clearly elevated when compared to their lean littermates (4−5%). These values are in line with those recorded for human diabetic patients and nondiabetic control subjects, respectively. In the study at hand, six weeks of once-daily treatment with a 100 mg/kg dose of **16c**β reduces HbA_{1c} by 4.7% units, or more than 80% of the difference between lean and diabetic animals. This result is clearly superior to that resulting from treatment with a maximal dose (500 mg/kg) of metformin in the same model (data not shown).

16cβ produces desirable changes in other relevant metabolic parameters as well. Like many human Type 2 diabetics, ob/ob mice have elevated levels of several key plasma lipids, including cholesterol, triglycerides, and free fatty acids (FFAs). These elevations are suppressed by treatment with **16c**β at 100 mg/kg orally. Serum cholesterol decreases by 60 mg/dL, though it does not return to lean levels; circulating free fatty acids are normalized, and triglyceride concentrations drop below those of the control group. These changes, which are consistent with a reduction in hepatic glucocorticoid signaling,[30] occur in the absence of significant weight loss. All are expected to provide additional benefit to the typical Type 2 diabetic patient.

The side effect profile of **16c**β is addressed by comparing it with **1** in a hypothalamic−pituitary−adrenal (HPA) activation model, which measures the normal response of the body to reduced glucocorticoid signaling. In this model, normal mice receive a single oral dose of antagonist and are examined 2 h later to determine the status of their HPA axis. As shown in Figure 7, a systemic glucocorticoid antagonist like **1** stimulates production of adrenocorticotrophic hormone (ACTH) by the pituitary; this elevation in ACTH then drives increased production of corticosterone from the adrenal glands. While **1** causes substantial increases in both parameters (~7-fold) in a dose-responsive fashion, even higher doses of **16c**β leave ACTH and corticosterone values unchanged at baseline levels. Importantly, the levels of the hormones remain unaltered at doses that demonstrated glucose-lowering activity in the ob/ob mouse. Thus, it appears that **16c**β demonstrates a significant degree of functional hepatic selectivity in clinically relevant models demonstrating antidiabetic efficacy and systemic antiglucocorticoid side effects.[31] The overall pharmacology profile of this agent indicates that it might be useful for treating Type 2 diabetes through the reduction of hepatic glucose production and that it is amenable to long-term dosing with a minimized mechanism-based side effect profile.

The Role of Bile Acid Transport. The bile acid component of **16c**β clearly plays a key role in targeting the antiglucocorticoid activity of this conjugate molecule to the liver. This observation would seem to confirm our initial hypothesis regarding the role of bile acid transporters in moving these conjugates selectively through the enterohepatic loop. However, additional studies probing this issue further have generated conflicting results. We note several of these below; in the end we find ourselves unable to reach a clear conclusion regarding the specific role of transporters in moving these molecules.

1. *The pharmacokinetic profile of* ***16c***β *is quite different from a typical bile acid*. One primary motivation for

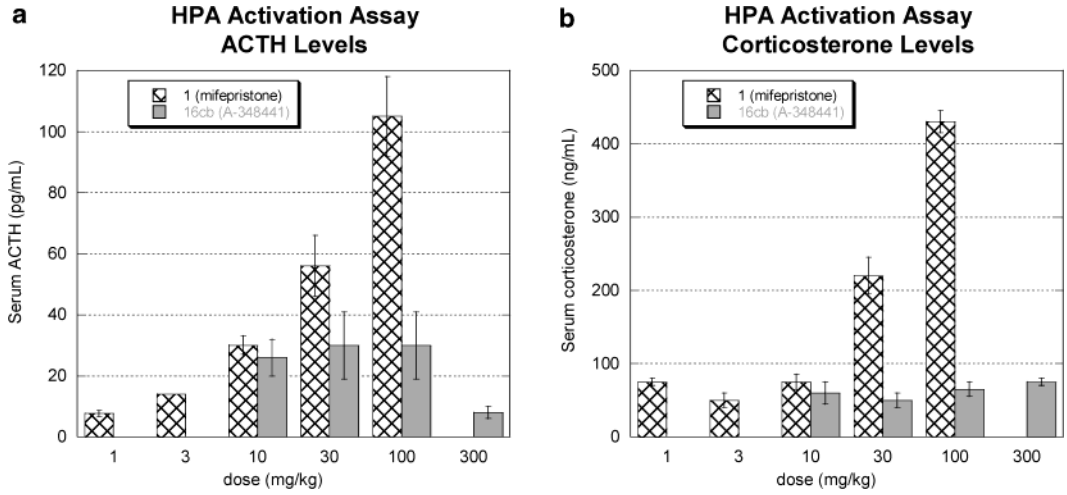

Figure 7. Comparison of A-348441 (**16c**β) with mifepristone (**1**) in the hypothalamic−pituitary−adrenal activation (HPA) model. A single oral dose of each agent is given to normal Sprague−Dawley rats (N = 10/group); measurements of ACTH (a) and corticosterone levels (b) are recorded 2 h postdose.

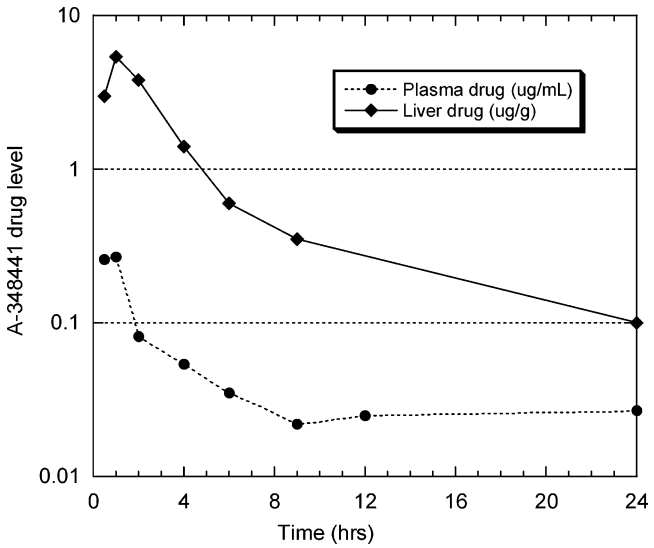

Figure 8. Plasma and liver concentrations following oral dosing of A-348441 (10 mg/kg) in ob/ob mice. Note: each data point represents a single animal.

our decision to use bile acids as a targeting device is the high efficiency with which they are constrained within the enterohepatic system. Steady-state kinetic analysis[18] has determined that the bulk absorption efficiency of bile acids during a single pass though the intestine is 97−99% ($F_A \sim 0.98$); similarly the efficiency of hepatic capture of cholic acid from the portal circulation is >90% ($F_H < 0.1$). As a result, the bile acid pool is highly conserved, with <1% of the total excreted daily despite multiple passes through the enterohepatic loop. By comparison,[33] segmental absorption and hepatic extraction studies of **16c**β indicate that the single-pass intestinal absorption efficiency is 20−30% ($F_A \sim 0.25$), and that the hepatic capture efficiency is ∼50% ($F_H \sim 0.5$). Thus, the systemic oral bioavailability ($F = F_A$*[1 − F_H]) of this compound is relatively low, at 10−15%; though liver levels are substantially higher (Figure 8). As a consequence, >98% of the drug dose is excreted within 24 h, largely through the bile. The absence of an efficient enterohepatic recirculation mechanism makes **16c**β distinctly different from a typical bile acid.

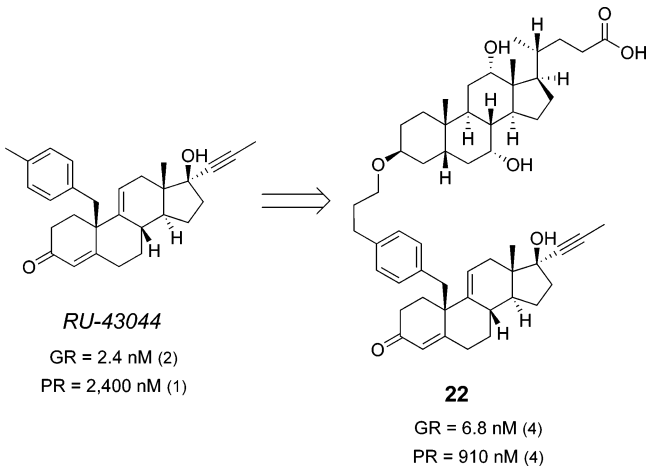

Figure 9. Bile acid conjugation of RU-43044, a selective GR antagonist.

2. *The address-and-message concept inherent in the design of* **16c**β *is not generally applicable.* Two sets of examples are relevant. (a) Numerous naturally occurring bile acids are able to engage the transporter systems in a manner similar to cholic acid. We expected that replacement of the cholic acid component of **16c**β with these alternative bile acids would lead to other analogues with similar in vivo properties. In practice this has proven not to be the case. Of particular note is the taurocholate conjugate **21b**. While taurocholic acid is one of the most efficient substrates for the bile acid specific transporters, **21b** has no beneficial effect in a rat prednisolone challenge experiment; and no drug can be detected in the liver after oral dosing. (b) Replacement of the mifepristone-derived fragment of **16c**β is also not tolerated. In an attempt to prepare an analogue of **16c**β that lacked affinity for the progesterone receptor, we conjugated the known GR-selective steroid RU-43044 using the same β-ether linkage to give **22** (Figure 9). This compound retains most of the potency and GR-selectivity of the parent but despite this has no activity in the rat prednisolone challenge model (see Table 1). These experiments make it clear that it is naïve to interpret the pharmacology of these bile acid-conjugated

GR antagonists purely in the context of our original address-and-message hypothesis.

Conclusions

Through a strategy of bile acid conjugation, it has been possible to prepare molecules that are potent inhibitors of glucocorticoid binding in vitro, demonstrate GR antagonist activity in cellular assays, and are selective for hepatic versus systemic glucocorticoid blockade in several animal models. The optimization of these properties requires compound screening in both in vitro and in vivo models and is facilitated by information from an X-ray crystallographic study of mifepristone binding to a GR fragment. From this analysis, conjugate **16c**β (A-348441) has been selected for in-depth evaluation as an antidiabetic agent acting through the reduction of hepatic glucose output.

The ability of **16c**β to lower plasma glucose levels in diabetic ob/ob mice *provides the first direct evidence that hepatic glucocorticoid blockade is sufficient to suppress hepatic glucose production*. While this hypothesis was central to our efforts in this area, the absence of a liver-selective agent has made it impossible to prove until now. The glucose-lowering effect of **16c**β persists throughout the day, even when the drug is given once-daily, and is reflected in profound changes in HbA1c levels, which provide the best assessment of long-term glycemic control. In addition, the compound reduces the hyperlipidemia that is often associated with Type 2 diabetes. As such, it presents a compelling profile as a novel treatment for diabetes and the metabolic syndrome.

Experimental Section

Abbreviations. 9-BBN, 9-borabicicylo[3.3.1]nonane; DBU, 1,8-diazabicyclo[5.4.0]undec-7-ene; DMAP, 4-(dimethylamino)-pyridine; DMF, dimethylformamide; EtOAc, ethyl acetate; KOtBu, potassium *tert*-butoxide; NBS, *N*-bromosuccinimide; PPh_3, triphenylphosphine; TBTU, *O*-(1*H*-benzotriazol-1-yl)-*N*,*N*,*N*′,*N*′-tetramethyluronium tetrafluoroborate; TFA, trifluoroacetic acid; TPAP, tetra-*n*-propylammonium perruthenate.

Compound Preparation. Unless otherwise specified, all solvents and reagents were obtained from commercial suppliers and used without further purification. All reactions were performed under nitrogen atmosphere unless specifically noted. Normal-phase flash chromatography was done using Merck silica gel 60 (230−400 mesh) from E. M. Science or was performed on a hybrid system employing Gilson components and Biotage prepacked columns. Reversed-phase chromatography was performed using a Gilson 215 solvent handler-driven HPLC system with a Zorbax SB-C18, 5 μm 21.2 × 250 mm column attached or using a Waters system with a Zorbax SB-C8, 5 μm 20 × 250 mm column. ^{1}H NMR spectra were recorded at 300 and 500 MHz; all values are referenced to tetramethylsilane as internal standard and are reported as shift (multiplicity, coupling constants, proton count). Mass spectral analysis is accomplished using fast atom bombardment (FAB-MS), electrospray (ESI-MS), or direct chemical ionization (DCI-MS) techniques. Analytical LC-MS was performed on a Shimadzu HPLC system with a Zorbax SB-C8, 5 μm 2.1 × 50 mm (Agilent technologies) column, with a PE Sciex, API 150EX single quadropole mass spectrometer, at a flow rate of 1 mL/min (0.05% NH_4OAc-buffer:MeCN and 0.05% HCOOH in H_2O:MeCN). All elemental analyses are consistent with theoretical values to within ±0.4% unless indicated.

Method A. Demethylation/Acetylation of Mifepristone. Method A1. To a solution of (11β,17α)-17-hydroxy-11-(4-(dimethylamino)phenyl)-17-prop-1-ynylestra-4,9-dien-3-one (**1**, mifepristone; 2.0 g, 4.7 mmol) in CH_2Cl_2 (10 mL) was added a filtered solution of NMO (2.6 g, 22 mmol) in CH_2Cl_2 (10 mL) which had been dried over Na_2SO_4. The resultant solution was stirred under nitrogen atmosphere in an ice bath. A solution of TPAP (160 mg) in CH_2Cl_2 (2 mL) was added dropwise over 10 min. The resultant solution was stirred at 0 °C for 20 min; reaction was quenched by addition of 10% sodium bisulfite (20 mL). The solution was warmed to room temperature and stirred an additional 10 min, then the product was partitioned between EtOAc and water. The aqueous layer was back-extracted with EtOAc; the combined organics were washed with pH 7 phosphate buffer and brine. The organic layer was filtered through Celite; the filtrate was concentrated in vacuo and the product precipitated. The product was filtered and dried to give 1.3 g (63%) of formamide.

Method A2. The crude formamide was dissolved in methanol (25 mL); 20 mL of 10% aqueous HCl was added slowly, and the resultant reaction mixture stirred at ambient temperature for 40 h. The pH of the reaction mixture was adjusted to pH 7 by slow addition of 10% Na_2CO_3 solution; a solid product precipitates. The product was isolated by filtration, dissolved in CH_2Cl_2 (20 mL), and dried over Na_2SO_4. The solvent was removed in vacuo to give 1.1 g (86%) of **2** as a white solid.

Method A3. A sample of this material (0.050 g, 0.12 mmol) in pyridine (1 mL) was treated with acetic anhydride (0.014 g, 0.14 mmol) and heated at 60 °C for 2 h. The reaction was cooled to room temperature and solvent was removed in vacuo. The residue was dissolved in 1.5 mL of a 1:1 mixture of DMSO/MeOH and purified by preparative reversed-phase HPLC (CH_3CN/H_2O) to give **3**.

Method B. Preparation of Cholic Acid Aspartamide 4. Method B1. A solution of compound **2** (0.90 g, 2.2 mmol) and *N*-*tert*-butoxycarbonylglutamic acid methyl ester (0.63 g, 2.4 mmol) in DMF (10 mL) was cooled at 0 °C; diisopropylethylamine (0.83 mL, 4.8 mmol), and TBTU (0.77 g, 2.4 mmol) were added sequentially. The reaction was allowed to reach room temperature, and the stirring was continued for 2 days. The mixture was poured into ice−water with stirring. The precipitate was filtered and washed with water. The dried solid was purified by silica gel chromatography (2−5% MeOH/CH_2Cl_2) to give 0.93 g of the desired product **4**.

Method B2. The above compound (0.92 g, 1.4 mmol) was treated with freshly prepared saturated HCl/EtOAc for 1 h, until no starting material remained when monitored by TLC. All volatile materials were removed under vacuum to give 0.75 g the desired product as a yellowish solid. The crude product (0.74 g, 1.2 mmol) was combined with cholic acid (0.65 g, 1.6 mmol) in DMF (10 mL); the resultant solution was cooled to 0 °C, and diisopropylethylamine (0.83 mL, 4.8 mmol) and TBTU (0.51 g, 1.6 mmol) were added. The reaction was allowed to reach room temperature, and the stirring was continued for 2 days. The mixture was poured into ice−water with stirring. The precipitate was filtered, washed with water, and dried. The residue was purified by silica gel column (5−10% MeOH/CH_2Cl_2) to give 0.29 g of a yellowish solid. This material (0.29 g, 0.30 mmol) was treated with aqueous lithium hydroxide (2 M, 8 mL) and THF (8 mL) for 2 h, until no starting material remained as monitored by TLC. All solvents were removed in vacuo, and the residue was purified by silica gel chromatography (10−15% MeOH/CH_2Cl_2, in the presence of 2% acetic acid) to give 0.23 g of **15**.

Method C. Preparation of Carbamate-Linked Derivatives of Cholic Acid. Method C1. Preparation of compound **5**. To a solution of cholic acid methyl ester (2.0 g, 4.7 mmol) stirring in pyridine (5 mL) at 0 °C was added 4-nitrophenyl-chloroformate (1.4 g, 7.1 mmol). The mixture was stirred at 0 °C for 30 min and at room temperature for 1 h. The reaction mixture was partitioned between EtOAc (50 mL) and 1 N HCl (50 mL). The aqueous layer was extracted with EtOAc (3 × 30 mL). The combined organic layers were washed with brine (50 mL), dried over $MgSO_4$, and concentrated in vacuo. The crude carbonate was dissolved in 1,4-dioxane (5 mL) and water (5 mL) and was treated with ethanolamine (0.58 g, 9.5 mmol) and 4-methylmorpholine (0.96 g, 9.5 mmol). The mixture was

stirred at 50 °C for 16 h. The reaction mixture was partitioned between EtOAc (20 mL) and 1 N HCl (20 mL). The aqueous layer was extracted with EtOAc (3 × 20 mL). The combined organic layers were washed with brine (15 mL), dried over $MgSO_4$, and concentrated in vacuo. A portion of the resultant alcohol (0.45 g, 0.80 mmol) was dissolved in DMF (5 mL) at 0°C; PPh_3 (0.32 g, 1.2 mmol) was added, followed by NBS (0.22 g, 1.2 mmol). The mixture was stirred at 0 °C for 1 h and at room temperature for 2 h. The reaction mixture was partitioned between EtOAc (10 mL) and 1 N HCl (10 mL). The aqueous layer was extracted with EtOAc (3 × 10 mL). The combined organic layers were washed with brine (15 mL), dried over $MgSO_4$, and concentrated in vacuo. The crude material was purified by flash chromatography on silica gel eluting with 20% acetone/hexanes and yielded bromide **5** as a white solid (0.31 g).

Method C2. Preparation of Compound 6. To a solution of the crude carbonate described in Method C1 (0.50 g, 0.85 mmol) in 1,4-dioxane (2 mL) and water (2 mL) were added glycine (0.13 g, 1.7 mmol) and 4-methylmorpholine (0.17 g, 1.7 mmol). The mixture was stirred at 50 °C for 16 h. The reaction mixture was partitioned between EtOAc (10 mL) and 1 N HCl (10 mL). The aqueous layer was extracted with EtOAc (3 × 10 mL). The combined organic layers were washed with brine (15 mL), dried over $MgSO_4$, and concentrated in vacuo to yield acid **6** as a light yellow oil.

Method C3. Preparation of Compound 10. To a solution of cholic acid methyl ester (4.0 g, 9.5 mmol) in pyridine (10 mL) were added DMAP (1.3 g, 10 mmol) and acetic anhydride (1.1 g, 10 mmol). The mixture was stirred at 0 °C for 2 h and at room temperature for 8 h. The reaction mixture was partitioned between EtOAc (50 mL) and 1 N HCl (50 mL). The aqueous layer was extracted with EtOAc (3 × 30 mL). The combined organic layers were washed with brine (50 mL), dried over $MgSO_4$, and concentrated in vacuo. The crude product, a light yellow solid, was dissolved in pyridine (15 mL) at 0 °C and treated with 4-nitrophenylchloroformate (2.1 g, 10 mmol). The reaction was stirred at 0 °C for 30 min and at room temperature for 1 h. The reaction mixture was partitioned between EtOAc (50 mL) and 1 N HCl (50 mL). The aqueous layer was extracted with EtOAc (3 × 30 mL). The combined organic layers were washed with brine (50 mL), dried over $MgSO_4$, and concentrated in vacuo. The crude carbonate was dissolved in 1,4-dioxane (15 mL) and water (15 mL) and was treated with ethanolamine (1.2 g, 19 mmol) and 4-methylmorpholine (1.9 g, 19 mmol). The reaction was stirred at 50 °C for 16 h. The reaction mixture was partitioned between EtOAc (50 mL) and 1 N HCl (50 mL). The aqueous layer was extracted with EtOAc (3 × 20 mL). The combined organic layers were washed with brine (50 mL), dried over $MgSO_4$, and concentrated in vacuo. The crude material was purified by flashing chromatography on silica gel eluting with 40% acetone/hexanes and yielded the alcohol as a white solid (2.6 g, 50% yield over three steps). Reaction of the alcohol under the NBS/PPh_3 conditions described above yielded the corresponding bromide **10** (1.2 g, 45% yield).

Method C4. Preparation of Compound 12. To a solution of the crude carbonate described in Method C3 (0.50 g, 0.79 mmol) in 1,4-dioxane (2 mL) and water (2 mL) were added glycine (0.13 g, 1.7 mmol) and 4-methylmorpholine (0.17 g, 1.7 mmol). The reaction was stirred at 50 °C for 16 h. The reaction mixture was partitioned between EtOAc (10 mL) and 1 N HCl (10 mL). The aqueous layer was extracted with EtOAc (3 × 10 mL). The combined organic layers were washed with brine (15 mL), dried over $MgSO_4$, and concentrated in vacuo, yielding crude acid **12** as a light yellow oil.

Method C5. Preparation of Compound 13. To a solution of cholic acid methyl ester (4.0 g, 9.5 mmol) in pyridine (10 mL) were added DMAP (2.5 g, 21 mmol) and acetic anhydride (2.1 g, 21 mmol). The reaction was stirred at 0 °C for 2 h and at room temperature for 8 h. The reaction mixture was partitioned between EtOAc (50 mL) and 1 N HCl (50 mL). The aqueous layer was extracted with EtOAc (3 × 30 mL). The combined organic layers were washed with brine (50 mL), dried over $MgSO_4$, and concentrated in vacuo, yielding the C3-/C7-diacetate as a light yellow solid. This material was dissolved in pyridine (15 mL) at 0 °C and was treated with 4-nitrophenylchloroformate (2.1 g, 10 mmol). The reaction was stirred at 0 °C for 30 min and at room temperature for 1 h. The reaction mixture was partitioned between EtOAc (50 mL) and 1 N HCl (50 mL). The aqueous layer was extracted with EtOAc (3 × 30 mL). The combined organic layers were washed with brine (50 mL), dried over $MgSO_4$, and concentrated in vacuo. The resultant crude carbonate **24** was dissolved in 1,4-dioxane (15 mL) and water (15 mL) and was treated with glycine (1.4 g, 19 mmol) and 4-methylmorpholine (1.9 g, 19 mmol). The reaction was stirred at 50 °C for 16 h. The reaction mixture was partitioned between EtOAc (50 mL) and 1 N HCl (50 mL). The aqueous layer was extracted with EtOAc (3 × 20 mL). The combined organic layers were washed with brine (50 mL), dried over $MgSO_4$, and concentrated in vacuo, yielding crude acid **13** as a yellow oil.

Method D. Preparation of Amine-Linked Derivatives of Cholic Acid. Method D1. Preparation of Compound 9a. 3-Oxo-cholic acid methyl ester, prepared according to the method of Tserng[26] (550 mg, 1.3 mmol), was dissolved in 10 mL of acetonitrile and stirred with 5.0 mL of 2.0 M methanolic methylamine for 30 min at ambient temperature. 110 mg (1.6 mmol) of $NaCNBH_3$ was added, and stirring was continued for 2 h at room temperature. 5 drops of acetic acid was added; stirring was continued for an additional 1h, until TLC indicated that no starting ketone remained. 10 mL of water was added; the resultant mixture was extracted with ethyl acetate and dried over Na_2SO_4. This crude product (540 mg, 95%) was carried forward without further purification. 300 mg (0.69 mmol) of the crude amine is combined with 3 equiv of Hunig's base and 130 mg (0.69 mmol) of 4-bromobutyryl chloride in acetonitrile (6.0 mL); the resultant mixture was stirred overnight in a sealed bottle at ambient temperature. The resultant solution was carried forward without workup or purification.

Compounds **9b** and **9c** are prepared using the above procedures, substituting 2-bromoethyl isocyanate or 3-bromopropanesulfonyl chloride for 4-bromobutyryl chloride.

Method E. Preparation of Ether-Linked Derivatives of Cholic Acid. Method E1. Preparation of Compound 8a. A solution of 1.4 g (3.0 mmol) of 7α,12α-dihydroxy-3α-2-hydroxyethoxy-5β-cholanic acid (prepared according to the methods of Wess et al.[19]) in 5 mL of DMF, stirring at 0 °C, was treated with PPh_3 (0.63 g, 3.7 mmol) followed by the addition of NBS (0.95 g, 3.7 mmol). The mixture was stirred at 0 °C for 1 h and at ambient temperature for 2 h. The reaction mixture was partitioned between EtOAc (20 mL) and 1 N HCl (20 mL). The aqueous layer was extracted with EtOAc (3 × 20 mL). The combined organic layers were washed with brine (50 mL), dried over $MgSO_4$, and concentrated in vacuo. The crude material was purified by flash chromatography on silica gel eluting with 20% acetone/hexanes and yielded bromide **8a** as a white solid (0.95 g, 74% yield).

Method E2. Preparation of compound **8b**. A mixture of 7α,12α-dihydroxy-3α-2-hydroxyethoxy-5β-cholanic acid (prepared according to the methods of Wess et al.[19]) (7.1 g, 13 mmol), DMF (20 mL) and allyl bromide (20 mL, 230 mmol) was heated to 120 °C for 16 h. The reaction mixture was partitioned between EtOAc (100 mL) and 1 N HCl (100 mL). The aqueous layer was extracted with EtOAc (3 × 100 mL). The combined organic layers washed with brine (150 mL), dried over $MgSO_4$, and concentrated in vacuo. The crude product was dissolved in water (10 mL) and diethyl ether (10 mL) and treated with osmium tetroxide (30 mg) and sodium periodate (5.4 g, 25 mmol). The mixture was stirred at ambient temperature for 16 h. The reaction mixture was partitioned between EtOAc (50 mL) and sodium thiosulfate (2 M solution, 50 mL). The aqueous layer was extracted with EtOAc (3 × 10 mL). The combined organic layers were washed with brine (50 mL), dried over $MgSO_4$, and concentrated in vacuo. The crude material was purified by flash chromatography on silica gel eluting with 20% acetone/hexanes and yielded the aldehyde

as a white solid (6.4 g, 85% yield over two steps). The aldehyde was combined with sodium borohydride (0.54 g, 14 mmol) in THF (30 mL) and ethanol (10 mL) at ambient temperature. After stirring overnight, the reaction mixture was concentrated in vacuo and the crude alcohol was purified by flash chromatography on silica gel eluting with 40% acetone/hexanes. The resultant alcohol (4.3 g, 61% yield) was converted to the corresponding bromide **8b** using the procedures of Method E1.

Method E3. Preparation of Compound 7a. A solution of 7α,12α-dihydroxy-3β-2-hydroxyethoxy-5β-cholanic acid (prepared according to the methods of Wess et al.[19]) (2.5 g, 5.4 mmol) in DMF (10 mL) at 0 °C was treated with PPh_3 (2.1 g, 8.0 mmol) followed by the addition of NBS (1.4 g, 8.0 mmol). The mixture was stirred at 0 °C for 1 h and at ambient temperature for 2 h. The reaction mixture was partitioned between EtOAc (20 mL) and 1 N HCl (20 mL). The aqueous layer was extracted with EtOAc (3 × 20 mL). The combined organic layers were washed with brine (50 mL), dried over $MgSO_4$, and concentrated in vacuo. The crude material was purified by flash chromatography on silica gel eluting with 20% acetone/hexanes and yielded bromide **7a** as a white solid (2.2 g, 79% yield).

Compounds **7b**, **7c**, and **7d** are also prepared according to method E3, by substituting chenodeoxycholic, lithocholic, and deoxycholic acid methyl esters for cholic acid methyl ester in the procedure of Wess et al.[19] Compounds **7e** and **7f** are also prepared according to Method E3, by substituting propylene glycol and diethylene glycol for ethylene glycol in the procedure of Wess et al.[19]

Method F. Preparation of Compound 11. A solution of allyl iodide (10 mL, 110 mmol) in dry THF (45 mL) was dropwise added to commercial zinc-dust (7.5 g, 110 mmol) at ambient temperature and stirred for 90 min. A solution of 3-oxo-cholic acid methyl ester (16 g, 38 mmol) in dry THF (45 mL) was added slowly; the resultant mixture was stirred at ambient temperature for 3 days. Some water was added; the mixture was filtered and concentrated. The residue was taken up in EtOAc and partitioned with water; the organic layer was washed with brine and dried over Na_2SO_4. The crude product was purified by flash chromatography on silica gel, eluting with 1:1 EtOAc/*n*-heptane, to yield a white solid. The stereochemistry of addition (allyl group on β-face) was confirmed by NOE studies. The resultant triol (11 g, 23 mmol) was combined with imidazole (7.8 g, 110 mmol) in dry DMF (150 mL) and flushed with dry nitrogen. Trimethylsilyl chloride (12 mL, 92 mmol) was added, and the mixture was stirred overnight at ambient temperature. Some water was added and the reaction mixture was concentrated in vacuo. The residue was taken up in EtOAc/Et_2O (1:1), diluted with water, and extracted, and the organic layer was dried over Na_2SO_4 then concentrated. The crude product was purified by flash chromatography (dichloromethane/*n*-heptane 4:6) to afford the tris-silyl ether as a clear oil. This material (0.61 g, 0.90 mmol) was dissolved in dry THF (10 mL); 9-BBN (0.5 M in THF, 3.7 mL, 1.8 mmol) was added dropwise, and the resultant solution was stirred at ambient temperature until hydroboration was nearly complete, as judged by TLC. The reaction was cooled in a water bath; a mixture of aq KOH (5 mL, 9.0 mmol) and aq H_2O_2 (1.8 mL, 27 mmol) was added slowly, keeping the reaction temperature below ambient. After 30 min, the mixture was diluted with water and pH adjusted to ∼7 with sat. NH_4Cl followed by extraction with dichloromethane. The organic layer was concentrated *in* vacuo. The crude product was purified by flash chromatography on silica gel (EtOAc/*n*-heptane, gradient 0:1−3:7) to afford the alcohol as a clear oil. This material (1.0 g, 1.4 mmol) was dissolved in dry dichloromethane (25 mL) and cooled to 0 °C. DMAP (cat.) and triethylamine (2.0 mL, 14 mmol) were added, followed by *p*-toluenesulfonyl chloride (0.55 g, 2.9 mmol) added portionwise over 2 h. After 5 h stirring, the reaction was quenched with sat. aqueous NH_4Cl and water, followed by extraction with dichloromethane. After solvent removal in vacuo, the crude product was purified by flash chromatography on silica gel, eluting with EtOAc/*n*-heptane 1:9 to obtain tosylate **11** as a clear oil. The product was used immediately in the next reaction step.

Method G. Preparation of compound **14**. 3-Oxo-cholic acid methyl ester, prepared according to the method of Tserng[26] (17 g, 39 mmol), was dissolved in 125 mL of dichloromethane; 17 mL of Hünig's base was added with stirring, followed the slow addition of 8.7 mL (110 mmol, 3 eq) of chloromethyl methyl ether. The resultant mixture was warmed overnight at 45 °C. Solvents were removed in vacuo; the residue was partitioned between EtOAc and aqueous 1 N H_3PO_4. The organic phase was washed with brine, dried over Na_2SO_4, and concentrated. The crude product was purified by silica gel chromatography (gradient elution with 25% to 35% ethyl acetate/hexane) to afford the bis-MOM ether (17 g, 86% yield). A sample of this material (9.6 g) was dissolved in 100 mL of dry THF and cooled in an ice bath. Allyl bromide (2.3 mL) was added, followed by 2.6 g of KOtBu. The mixture was stirred for 90 min, then the reaction was quenched by addition of aqueous 1 N H_3PO_4. The mixture was extracted with EtOAc; the organic phase was washed with brine, dried over Na_2SO_4, and concentrated. The crude product was dissolved in 120 mL of MeOH, 1.1 g of $NaBH_4$ pellets was added, and the resultant mixture was stirred at ambient temperature for 4 h. Solvents were removed in vacuo; the residue was partitioned between EtOAc and aqueous 1 N H_3PO_4. The organic phase was washed with brine, dried over Na_2SO_4, and concentrated. The crude product was purified by silica gel chromatography (gradient elution with 33% to 40% ethyl acetate/hexane). The resultant C3α-alcohol was dissolved in 50 mL of dichloromethane; 5 mL of Hünig's base was added with stirring, followed the slow addition of 1.8 mL of chloromethyl methyl ether. The resultant mixture was warmed for 3 h at 45 °C. Solvents were removed in vacuo; the residue was partitioned between EtOAc and water. The organic phase was washed with brine, dried over Na_2SO_4, and concentrated. The crude product was purified by silica gel chromatography (25% ethyl acetate/hexane) to afford the tris-MOM ether (3.8 g). To a well-stirred solution of this compound (1.2 g, 2.0 mmol) in diglyme (4 mL) at 0 °C was added borane−THF solution (0.66 mL, 1.0 mmol). The resultant solution was stirred at 0 °C for 1 h and warmed to ambient temperature for 3 h. The reaction mixture was then reacted with trimethylamine *N*-oxide dihydrate (0.44 g, 4.0 mmol) at 60 °C for 2 h and 70 °C overnight. The mixture was partitioned between H_2O and EtOAc. The organic layer was washed with brine, dried over Na_2SO_4, and concentrated. The crude product was purified by silica gel chromatography (50% ethyl acetate/hexane) to afford the corresponding alcohol (0.80 g, 66% yield). A sample of this compound (20 mg, 0.033 mmol) in acetonitrile (0.5 mL) was stirred overnight at ambient temperature with methanesulfonyl chloride (4.5 mg, 0.039 mmol) and Hunig's base (30 mg, 0.23 mmol). The resultant solution was used in subsequent procedures without further workup or purification.

Method H. Coupling of Fragments. Method H1. Acylation-Based Couplings. Preparation of Compound 16αa. To a solution of acid **6** (0.53 g, 1.0 mmol) in DMF (5 mL) was added compound **2** (0.50 g, 1.2 mmol), followed by TBTU (0.48 g, 1.5 mmol). The mixture was warmed to 50 °C for 5 h. The reaction mixture was partitioned between EtOAc (20 mL) and 1 N HCl (20 mL). The aqueous layer was extracted with EtOAc (3 × 20 mL). The combined organic layers were washed with brine (20 mL), dried over $MgSO_4$, and concentrated in vacuo. The crude product was dissolved in 1,4-dioxane (5 mL) and was treated with aqueous LiOH solution (2 M, 2 mL); the resultant mixture was stirred at ambient temperature for 16 h. The reaction mixture was partitioned between EtOAc (10 mL) and 1 N HCl (30 mL or until acidic). The aqueous layer was extracted with EtOAc (3 × 10 mL). The combined organic layers were washed with brine (20 mL), dried over $MgSO_4$, and concentrated in vacuo. The crude product was purified with reversed phase HPLC (Zorbax XDB-C_{18}, 21.2 × 250 mm, water/acetonitrile/0.1% TFA) and yielded conjugate **16αa**.

Compounds **15**, **19a**, and **20** were also prepared according to method H1.

Method H2. Alkylation-Based Couplings. Preparation of Compound 16βc. A solution of bromide **7a** (1.0 g, 1.8 mmol) and compound **2** (0.87 g, 2.1 mmol) in acetonitrile (5 mL) in a dry pressure tube equipped with a stir bar was treated with sodium iodide (0.03 g, 0.20 mmol) and diisopropylethylamine (0.68 g, 5.23 mmol). The reaction was heated to 100 °C with an oil bath for 16 h. The reaction mixture was partitioned between EtOAc (20 mL) and 1 N HCl (20 mL). The aqueous layer was extracted with EtOAc (3 × 20 mL). The combined organic layers were washed with brine (50 mL), dried over $MgSO_4$, and concentrated in vacuo. The crude product was dissolved in 1,4-dioxane (10 mL) and was treated with LiOH solution (2M, 5 mL); the mixture was stirred at room temperature for 16 h. The reaction mixture was partitioned between EtOAc (50 mL) and 1 N HCl (100 mL or until acidic). The aqueous layer was extracted with EtOAc (3 × 20 mL). The combined organic layers were washed with brine (50 mL), dried over $MgSO_4$, and concentrated in vacuo. The crude product was purified with reversed phase HPLC (Zorbax XDB-C_{18}, 21.2 × 250 mm, water/acetonitrile/0.1% TFA) yielding conjugate **16βc**.

Compounds **16αb**, **16αc**, **16αd**, **16αe**, **16αf**, **16αh**, **16βg**, **16βh**, **16βi**, **16βj**, **16βk**, **17**, **18**, and **19b** were also prepared according to method H2.

Method I. Preparation of Glycocholate and Taurocholate Conjugates. Method I1. Preparation of Compound 21b. To a solution of compound **16βc** (10 mg, 0.01 mmol) in DMF (1 mL) were added TBTU (7 mg, 0.02 mmol) and taurine (3 mg, 0.02 mmol). The mixture was stirred at 50 °C for 1 h. The reaction mixture was partitioned between EtOAc (2 mL) and 1 N HCl (2 mL). The aqueous layer was extracted with EtOAc (3 × 2 mL). The combined organic layers were washed with brine (5 mL), dried over $MgSO_4$, and concentrated in vacuo. The crude product was purified with reverse phase HPLC (Zorbax XDB-C_{18}, 21.2 × 250 mm, water/acetonitrile/0.1% TFA) yielded 4 mg of compound **21b**.

Compound **21a** was prepared using method I.

Compound Characterization. Compound **3.** ^{1}H NMR (300 MHz, $CDCl_3$) δ 7.24 (d, J = 8.5 Hz, 1 H), 7.10 (d, J = 8.5 Hz, 1 H), 5.80 (s, 1 H), 4.44 (d, J = 6.2 Hz, 1 H), 3.26 (s, 3 H), 2.80 (dt, J = 7.0 Hz, 2.5 Hz, 1 H), 2.64−2.59 (m, 2 H), 2.50−2.10 (m, 6 H), 2.08−1.25 (m, 7 H), 1.91 (s, 3 H), 1.85 (s, 3 H), 0.50 (s, 3 H). MS (ESI(+)Q1) MS m/z 458 $(M + H)^+$. Anal. Calcd for $C_{30}H_{35}NO_3 \cdot 0.8\ H_2O$: C, 76.34; H, 7.82; N, 2.97. Found: C, 76.47; H, 7.88; N, 2.93. HRMS calcd for $C_{30}H_{36}NO_3$: 458.2695. Observed: 458.2698.

Compound 15. ^{1}H NMR (500 MHz, $CDCl_3$) δ 7.18−7.35 (2×d, 4H, arom.), 5.76 (s, 1H, H-4), 4.55 (d, 1H), 4.18 (d, 1H), 3.94 (s, 1H), 3.79 (s, 1H), 3.25 (s, 3H, NCH_3), 1.86 (s, 3H), 0.99 (d, 3H, CH_3), 0.92 (s, 3H, CH_3), 0.70 (s, 3H, CH_3), 0.49 (s, 3H). MS (ESI) m/z 936 $(M + 1)^+$. Anal. Calcd for $C_{57}H_{78}N_2O_9 \cdot 2.0\ H_2O$. 0.3 ETOAc: C, 70.06; H, 8.53; N, 2.81. Found: C, 69.85; H, 8.30; N, 2.96. HRMS calcd for $C_{57}H_{79}N_2O_9$: 935.5780. Found: 935.5785.

Compound 16αa. ^{1}H NMR (500 MHz, CD_3OD) δ 7.38 (d, J = 7.0 Hz, 2 H), 7.26 (d, J = 8.1 Hz, 2 H), 5.76 (s, 1 H), 4.56 (d, J = 6.6 Hz, 1 H), 4.36 (m, 1 H), 3.96 (m, 1 H), 3.79 (m, 1 H), 3.55 (m, 2 H), 3.23 (m, 3 H), 2.87 (m, 1 H), 2.54−2.74 (m, 3 H), 2.20−2.54 (m, 9 H), 2.17 (m, 2 H), 2.09 (m, 1 H), 1.77 (m, 6 H), 1.66 (m, 3 H), 1.55 (m, 6 H), 1.27−1.48 (m, 11 H), 1.25 (m, 3 H), 1.12 (m, 2 H), 1.02 (m, 5 H), 0.89 (m, 3 H), 0.80 (s, 3 H), 0.72 (s, 3 H); MS (ESI) m/z 924 $(M + NH_4)^+$; 905 $(M - H)^-$. Anal. Calcd for $C_{55}H_{74}N_2O_9 \cdot 1.0\ H_2O$: C, 71.40; H, 8.28; N, 3.03. Found: C, 71.54; H, 8.43; N, 3.08. HRMS calcd for $C_{55}H_{74}N_2O_9Na$: 929.5287. Found: 929.5281.

Compound 16αb. ^{1}H NMR (500 MHz, CD_3OD) δ 7.31 (d, J = 7.8 Hz, 2 H), 7.17 (m, 2 H), 5.75 (s, 1 H), 4.38 (m, 1 H), 3.94 (m, 1 H), 3.81 (m, 2 H), 3.39 (m, 2 H), 3.23 (m, 2 H), 3.12 (m, 2 H), 2.83 (m, 3 H), 2.66 (m, 2 H), 2.12−2.58 (m, 11 H), 1.62−2.12 (m, 16 H), 1.56 (m, 6 H), 1.45 (m, 4 H), 1.02 (m, 6 H), 1.02 (d, J = 6.6 Hz, 3 H), 0.93 (s, 3 H), 0.72 (s, 3 H), 0.50 (s, 3 H); MS (ESI) m/z 893 $(M + H)^+$ 891 $(M - H)^-$; HRMS calcd for $C_{55}H_{77}N2O_8$: 893.5674; found: 893.5649.

Compound 16αc. ^{1}H NMR (400 MHz, CD_3OD) δ 7.47 (s, 4 H), 5.76 (s, 1 H), 4.59 (d, J = 7.6 Hz, 1 H), 3.96 (t, J = 2.4 Hz, 1 H), 3.79 (q, J = 2.8 Hz, 1 H), 3.74 (m, 2 H), 3.71 (t, J = 5.2 Hz, 1 H), 3.32−3.53 (m, 2 H), 3.26 (m, 1 H), 2.68−3.09 (m, 4 H), 2.12−2.68 (m, 12 H), 1.86 (s, 3 H), 1.66−2.12 (m, 13 H), 1.21−1.66 (m, 14 H), 1.14 (m, 1 H), 1.03 (d, J = 6.6 Hz, 3 H), 0.89 (s, 3 H), 0.86 (m, 1 H), 0.72 (s, 3 H), 0.49 (s, 3 H); MS (ESI) m/z 850 $(M + H)^+$; HRMS calcd for $C_{54}H_{76}NO_7$: 850.5616; Found: 850.5606.

Compound 16αd. ^{1}H NMR (300 MHz, CD_3OD) δ 7.03 (d, J = 9 Hz, 2H), 6.70 (d, J = 9 Hz, 2H), 5.73 (s, 1H), 4.39 (d, J = 7.5 Hz, 1H), 4.97 (s, 2H), 4.80 (s, 2H), 3.35 (m, 2H), 2.88 (d, J = 4.5 Hz, 3H), 2.84 (d, J = 9 Hz, 3H), 2.65−1.05 (envelope, 46H), 1.85 (s, 3H), 1.03 (d, J = 6 Hz, 3H), 0.94 (d, J = 4.5 Hz, 3H), 0.72 (s,3H), 0.54 (s, 3H). MS (ESI) m/z 905 $(M + H)^+$. HRMS calcd for $C_{57}H_{81}N_2O_7$: 905.6038. Found: 905.6046.

Compound 16αe. ^{1}H NMR (300 MHz, CD_3OD) δ 7.02 (d, J = 9 Hz, 2H), 6.73 (d, J = 9 Hz, 2H), 5.72 (s, 1H), 4.48 (d, J = 7.5 Hz, 1H), 3.97 (s, 2H), 3.80 (s, 2H), 3.90 (m, 1H), 2.92 (s, 3H), 2.67 (s, 3H), 2.65−1.06(envelope, 46H), 1.85 (s, 3H), 1.03 (d, J = 6 Hz, 3H), 0.93 (s, 3H), 0.72 (s, 3H), 0.54 (s, 3H). MS (ESI) m/z 906 $(M + H)^+$. Anal. Calcd for $C_{56}H_{79}N_3O_7 \cdot 1.0\ H_2O$: C, 72.77; H, 8.83; N, 4.55. Found: C, 72.93; H, 9.07; N, 4.58. HRMS calcd for $C_{56}H_{80}N_3O_7$: 906.5991; Found: 906.5966.

Compound 16αf. ^{1}H NMR (300 MHz, CD_3OD) δ 7.05 (d, J = 9 Hz, 2H), 6.72 (d, J = 9 Hz, 2H), 5.73 (s, 1H), 4.40 (d, J = 7.5 Hz, 1H), 3.96 (s, 1H), 3.80 (s, 1H), 3.53−3.42 (m, 3H), 3.03 (t, J = 7.5 Hz, 2H), 2.88 (s, 3H), 2.85 (m, 1H), 2.79 (s, 3H), 2.66−1.67 (envelop, 33H), 1.59−1.27 (m, 14H), 1.03 (d, J = 6 Hz, 3H), 0.93 (s, 3H), 0.72 (s, 3H), 0.53 (s, 3H); MS(ESI) m/z 941 $(M + 1)^+$, 939 $(M - 1)^-$. Anal. Calcd for $C_{56}H_{80}N_2O_8S$. 1.0 EtOAc: C, 70.01; H, 8.62; N, 2.72. Found: C, 69.65; H, 8.58; N, 2.64. HRMS calcd for $C_{56}H_{81}N_2O_8S$: 941.5708; Found: 941.5715.

Compound 16αh. ^{1}H NMR (400 MHz, CD_3OD) δ 7.32−7.66 (m, 4 H), 5.77 (s, 1 H), 4.61 (m, 1 H), 3.96 (m, 2 H), 3.83 (m, 2 H), 3.73 (m, 3 H), 3.63 (m, 5 H), 3.53 (m, 5 H), 3.27 (m, 4 H), 2.85 (m, 2 H), 2.66 (m, 4 H), 2.50 (m, 3 H), 2.12−2.42 (m, 9 H), 1.92−2.12 (m, 2 H), 1.69−1.92 (m, 5 H), 1.58 (m, 7 H), 1.26−1.50 (m, 6 H), 1.13 (m, 2 H), 1.02 (d, J = 5.2 Hz, 3 H), 0.94 (s, 3 H), 0.72 (s, 3 H), 0.48 (s, 3 H); MS (ESI) m/z 894 $(M + H)^+$ 892 $(M - H)^-$; HRMS calcd for $C_{56}H_{80}NO_8$: 894.5878; Found: 894.5901.

Compound 16βc. ^{1}H NMR (500 MHz, CD_3OD) δ 7.07−7.71 (m, 4 H), 5.76 (s, 1 H), 4.57 (d, J = 7.8 Hz, 1 H), 3.95 (s, 1 H), 3.78 (d, J = 2.2 Hz, 1 H), 3.74 (t, J = 4.4 Hz, 1 H), 3.44 (m, 1 H), 3.23 (m, 3 H), 2.86 (m, 1 H), 2.66 (m, 1 H), 2.50 (m, 2 H), 2.16−2.41 (m, 7 H), 2.15 (m, 2 H), 2.08 (m, 1 H), 1.95 (m, 3 H), 1.85 (m, 5 H), 1.75 (m, 5 H), 1.57 (m, 7 H), 1.40 (m, 7 H), 1.31 (m, 6 H), 1.01 (d, J = 6.6 Hz, 3 H), 0.92 (m, 5 H), 0.71 (s, 3 H), 0.48 (s, 3 H); MS (ESI) m/z 850 $(M + H)^+$ 848 $(M - H)^-$; Anal. Calcd for $C_{54}H_{75}NO_7 \cdot 1.0\ H_2O$: C, 74.70; H, 8.94; N, 1.61. Found: C, 74.65; H, 8.58; N, 1.78. HRMS calcd for $C_{54}H_{76}NO_7$: 850.5616; found 850.5620:

Compound 16βg. ^{1}H NMR (400 MHz, CD_3OD) δ 6.92 (d, J = 8.5 Hz, 2 H), 6.86 (d, J = 8.0 Hz, 2 H), 5.28 (s, 1 H), 4.08 (m, 1 H), 3.74 (m, 1 H), 3.60 (m, 1 H), 3.47 (m, 1 H), 3.29 (m, 1 H), 3.13 (m, 2 H), 3.01 (m, 1 H), 2.91 (m, 2 H), 2.72 (m, 3 H), 2.25−2.45 (m, 1 H), 2.17 (m, 2 H), 2.02 (m, 3 H), 1.88 (m, 4 H), 1.72 (m, 4 H), 1.60 (m, 1 H), 1.48 (m, 4 H), 1.37 (m, 5 H), 1.24 (m, 6 H), 1.08 (m, 6 H), 0.78−1.00 (m, 12 H), 0.75 (m, 1 H), 0.65 (m, 1 H), 0.53 (d, J = 6.6 Hz, 3 H), 0.42 (s, 3 H), 0.23 (s, 3 H); MS (ESI) m/z 864 $(M + H)^+$ 862 $(M - H)^-$; HRMS calcd for $C_{55}H_{78}NO_7$: 864.5773; Found: 864.5751.

Compound 16βh. ^{1}H NMR (300 MHz, CD_3OD): δ 7.40 (bd s, 4H), 5.77 (s, 1H), 4.56 (d, J = 8 Hz, 1H), 3.96 (bd s, 1H), 3.80 (bd q, J = 3 Hz, 1H), 3.71 (m, 2H), 3.57 (bd s, 1H), 3.49 (bd s, 2H), 3.23 (s, 3H), 2.85 (dt, J = 6,15 Hz, 1H), 2.64 (m, 2H), 2.6−1.1 (envelope, 45H), 1.86 (s, 3H), 1.03 (d, J = 7 Hz, 3H), 0.92 (s, 3H), 0.73 (s, 3H), 0.48 (s, 3H). MS (ESI) m/z 894 $(M + H)^+$, m/z 892 $(M - H)^-$. HRMS calcd for $C_{54}H_{80}NO_8$: 894.5878. Found: 894.5893.

Compound 16βi. ^{1}H NMR (300 MHz, CD_3OD): δ 7.4−7.3 (m, 4H), 5.76 (s, 1H), 4.55 (d, J = 8 Hz, 1H), 3.95 (bd s, 1H), 3.71 (m, 2H), 3.49 (bd s, 1H), 3.21 (s, 3H), 2.85 (m, 1H), 2.64

(m, 2H), 2.6−2.4 (m, 3H), 2.4−1.2 (envelope, 41H), 1.86 (s, 3H), 1.00 (d, J = 7 Hz, 3H), 0.92 (s, 3H), 0.70 (s, 3H), 0.48 (s, 3H). MS (ESI) m/z 834 $(M + H)^+$, m/z 832 $(M - H)^-$. HRMS calcd for $C_{54}H_{76}NO_6$: 834.5667. Found: 834.5661.

Compound 16βj. ^{1}H NMR (300 MHz, CD_3OD): δ 7.42 (bd s, 4H), 5.76 (s, 1H), 4.57 (d, J = 8 Hz, 1H), 3.8−3.7 (m, 3H), 3.43 (bd s, 1H), 3.25 (s, 3H), 2.87 (m, 1H), 2.65 (m, 2H), 2.6−2.4 (m, 3H), 2.4−1.1 (envelope, 41H), 1.86 (s, 3H), 0.95 (d, J = 7 Hz, 3H), 0.93 (s, 3H), 0.69 (s, 3H), 0.47 (s, 3H). MS (ESI) m/z 834 $(M + H)^+$, m/z 832 $(M - H)^-$. HRMS calcd for $C_{54}H_{76}NO_6$: 834.5667. Found: 834.5666.

Compound 16βk. ^{1}H NMR (300 MHz, CD_3OD): δ 7.02 (d, J = 9 Hz, 2H), 6.70 (d, J = 9 Hz, 2H), 5.73 (s, 1H), 4.38 (d, J = 7 Hz, 1H), 3.6−3.5 (m, 7H), 2.95 (s, 3H), 2.92 (m, 1H), 2.65 (m, 2H), 2.6−1.1 (envelope, 41H), 1.86 (s, 3H), 0.94 (d, J = 7 Hz, 3H), 0.86 (s, 3H), 0.66 (s, 3H), 0.55 (s, 3H). MS (ESI) m/z 818 $(M + H)^+$, m/z 816 $(M - H)^-$. Anal. Calcd for $C_{54}H_{75}NO_5$: C, 79.27; H, 9.24; N, 1.71. Found: C, 79.06; H, 9.44; N, 1.68. HRMS calcd for $C_{54}H_{76}NO_5$: 818.5718. Found: 818.5729.

Compound 17. ^{1}H NMR (300 MHz, CD_3OD): δ 7.02 (d, J = 8.5 Hz, 2H), 6.66 (d, J = 8.5 Hz, 2H), 5.73 (s, 1H), 4.39 (d, J = 6.9 Hz, 1H), 3.96−3.92 (m, 1H), 3.81 − 3.76 (m, 1H), 3.26 (t, J = 7.3 Hz, 2H), 2.88 (s, 3H), 2.85−2.77 (m, 1H), 2.62 (m, 2H), 2.55−2.10 (m, 11H), 2.10−1.60 (m, 14), 1.86 (s, 3H), 1.60−1.24 (m, 15H), 1.16−1.05 (m, 1H), 1.01 (d, J = 6.0 Hz, 3H), 0.94 (s, 3H), 0.71 (s, 3H), 0.54 (s, 3H); MS (ESI) m/z $(M + H)^+$ 864, $(M - H)^-$ 862. Anal. Calcd for $C_{55}H_{77}NO_7 \cdot 0.5H_2O$: C, 75.66; H, 9.00; N,1.61. Found: C, 75.59; H, 9.32; N, 1.43.

Compound 18. ^{1}H NMR (300 MHz, $CDCl_3$) δ 6.93−7.05 (m, 2 H), 6.57−6.70 (m, 2 H), 5.76 (s, 1 H), 4.34 (d, J = 6.1 Hz, 1 H), 3.96 (m, 1 H), 3.83 (m, 1 H), 3.13−3.34 (m, 3 H), 2.89 (s, 3 H), 0.80−2.83 (m, 48 H), 1.90 (s, 3 H), 0.99 (d, J = 5.4 Hz, 3 H), 0.87 (s, 3 H), 0.69 (s, 3 H), 0.55 (s, 3 H); MS (ESI) m/z 864 $(M + H)^+$, 862 $(M - H)^-$. HRMS calcd for $C_{55}H_{77}NO_7$: 864.5773; found 864.5785.

Compound 19a. ^{1}H NMR (500 MHz, CD_3OD) δ 7.38 (d, J = 8.1 Hz, 1 H), 7.27 (d, J = 12.5 Hz, 2 H), 5.76 (s, 1 H), 4.66 (s, 1 H), 4.57 (s, 1 H), 4.57 (d, J = 6.6 Hz, 1 H), 4.56 (s, 1 H), 3.96 (s, 1 H), 3.59 (m, 1 H), 3.42 (m, 1 H), 3.25 (m, 2 H), 2.86 (m, 1 H), 2.52−2.73 (m, 3 H), 2.47 (m, 2 H), 2.33 (m, 5 H), 2.18 (m, 6 H), 2.08 (m, 2 H), 1.97 (m, 3 H), 1.80 (m, 10 H), 1.61 (m, 9 H), 1.31−1.52 (m, 7 H), 1.01 (d, J = 6.6 Hz, 3 H), 0.92 (s, 3 H), 0.71 (s, 3 H), 0.52 (s, 3 H); MS (ESI) m/z 907 $(M + H)^+$ 905 $(M - H)^-$; Anal. Calcd for $C_{55}H_{74}N_2O_9$ 0.0.6 TFA: C, 69.19; H, 7.71; N, 2.87. Found: 69.08; H, 7.60; N, 2.67.

Compound 19b. ^{1}H NMR (500 MHz, CD_3OD) δ 7.27 (m, 2 H), 7.10 (m, 2 H), 5.74 (s, 1 H), 4.72 (m, 1 H), 4.49 (m, 1 H), 3.97 (m, 1 H), 3.56 (m, 2 H), 3.44 (m, 2 H), 3.25 (m, 2 H), 3.15 (m, 3 H), 3.09 (m, 1 H), 2.85 (m, 2 H), 2.67 (m, 3 H), 2.48 (m, 3 H), 2.18−2.39 (m, 9 H), 1.90−2.13 (m, 9 H), 1.80 (m, 4 H), 1.60 (m, 5 H), 1.44 (m, 6 H), 1.28 (m, 6 H), 1.14 (m, 2 H), 1.01 (d, J = 6.6 Hz, 3 H), 0.93 (s, 3 H), 0.72 (s, 3 H), 0.51 (s, 3 H); MS (ESI) m/z 893 $(M + H)^+$ 891 $(M - H)^-$; Anal. Calcd for $C_{55}H_{76}N_2O_8$. 1.6 TFA: C, 64.99; H, 7.27; N, 2.60. Found: C, 64.82; H, 7.13; N, 2.62. HRMS calcd for $C_{55}H_{77}N_2O_8$: 893.5674. Found: 893.5653.

Compound 20. ^{1}H NMR (400 MHz, CD_3OD) δ 7.38 (d, J = 6.1 Hz, 2 H), 7.27 (d, J = 8.0 Hz, 2 H), 6.1 (m, 3 H), 5.76 (s, 1 H), 4.90 (m, 2 H), 4.58 (m, 1 H), 4.00 (m, 8 H), 3.84 (m, 3 H), 3.21 (m, 3 H), 2.41−2.69 (m, 4 H), 2.33 (m, 2 H), 2.17 (m, 5 H), 2.06 (m, 5 H), 1.95 (m, 6 H), 1.86 (m, 2 H), 1.75 (m, 2 H), 1.46−1.68 (m, 3 H), 1.39 (m, 3 H), 1.28 (m, 6 H), 0.80−1.02 (m, 4 H), 0.74 (m, 3 H), 0.34−0.61 (m, 3 H); MS (ESI) m/z 907 $(M + H)^+$ 905 $(M - H)^-)^-$; Anal. Calcd for $C_{55}H_{74}N_2O_9$. 0.5 TFA: C, 71.24; H, 8.00; N, 2.99. Found: C, 71.40; H, 6.74; N, 2.65.

Compound 21a. ^{1}H NMR (300 MHz, CD_3OD) δ 7.02 (d, J = 9 Hz, 2H), 6.70 (d, J = 9 Hz, 2H), 5.72 (s, 1H), 4.38 (d, J = 7.5 Hz, 1H), 3.94 (s, 1H), 3.75 (s, 1H), 3.55−3.97 (m, 5H), 2.95 (s, 3H), 2.85−1.24 (envelope, 49H), 1.03 (d, J = 6 Hz, 3H), 0.85-(s, 3H), 0.70 (s, 3H), 0.55 (s, 3H); MS (ESI) m/z 907$(M + 1)^+$, 905$(M - 1)^-$. Anal. Calcd for $C_{56}H_{78}N_2O_8 \cdot 1.8H_2O$: C, 71.58; H, 8.75; N, 2.98. Found: C, 71.53, H, 8.66; N, 3.09. HRMS calcd for $C_{56}H_{79}N_2O_8$: 907.5831. Found: 907.5834.

Compound 21b. ^{1}H NMR (500 MHz, CD_3OD) δ 7.55 (d, J = 9.0 Hz, 2 H), 7.50 (d, J = 8.7 Hz, 2 H), 5.77 (s, 1 H), 4.61 (m, 1 H), 3.95 (m, 1 H), 3.80 (m, 3 H), 3.59 (m, 2 H), 3.44 (m, 1 H), 2.97 (m, 2 H), 2.86 (m, 1 H), 2.64 (m, 2 H), 2.53 (m, 3 H), 2.39 (m, 4 H), 2.03−2.30 (m, 10 H), 1.96 (m, 6 H), 1.77 (m, 6 H), 1.46−1.68 (m, 7 H), 1.39 (m, 8 H), 1.27 (m, 3 H), 1.12 (m, 2 H), 1.02 (d, J = 6.6 Hz, 3 H), 0.94 (s, 3 H), 0.71 (s, 3 H), 0.47 (s, 3 H); MS (ESI) m/z 864 $(M + H)^+$, 862 $(M - H)^-$; HRMS calcd for $C_{56}H_{81}N_2O_9S$: 957.5657; Found: 957.5666.

In Vitro Compound Evaluation. For all replicated dose−response data recorded using the assays below, averages were computed as the geometric mean.

GR Binding Assay. ^{3}H-Dexamethasone (TRK 645, "^{3}H-dex") was purchased from Pharmacia Amersham, Uppsala, Sweden. Dexamethasone ("dex") was purchased from Sigma. The Costar 96-well polypropylene plates (3794 or 3365) were purchased from Life Technologies AB, Täby, Sweden. The GF/B filter (1450-521), filter cassette (1450−104), MeltiLex scintillating wax (1450-441), sample bag (1450-42), Microbeta 1450-PLUS and Microsealer 1495-021 were all purchased from Wallac Oy, Turkku, Finland. Human glucocorticoid receptors were extracted from Sf9 cells infected with a recombinant baculovirus transfer vector containing the cloned hGR gene. Recombinant baculovirus was generated utilizing the BAC-TO-BAC expression system (Life Technologies) in accordance to instruction from the supplier. The hGR coding sequences were cloned into a baculovirus transfer vector by standard techniques. The recombinant baculoviruses expressing hGR were amplified and used to infect Sf9 cells. Infected cells were harvested 48 h post infection. The receptors were extracted from the cell pellet with a phosphate buffer (1 mM EDTA, 20 mM KPO_4 (pH8), 8.6% Glycerol, 12 mM MTG, 20 mM Na_2-MoO_4). The concentration of hGR in the extract was measured via specific binding of ^{3}H-dexamethasone ("^{3}H-dex") with the G25-assay as described in J. Steroid Biochem. Molec. Biol. **50**, No. 5/6, 313-318, 1994 and estimated to approximately 25 nM. The extract was aliquoted and stored at −70 °C. Dilution series of the test compounds and dexamethasone ("dex") as reference were made from 10 mM (1 mM dex) stock solutions in DMSO. 10 μL of each dilution was added in duplicate to the wells. The cell extracts were diluted 10-fold in EPMo + MTG buffer (1 mM EDTA, HPO_4 20 mM (pH8), 6 mM MTG). The diluted extract was added to the wells (110 μL). ^{3}H-dex was diluted from the stock solution to 10 nM in EPMo + MTG buffer. 110 μL of the diluted ^{3}H-dex were added to the wells. The final concentration of hGR in the experiment was estimated to be 1 nM. All preparations were made in ambient temperature (20−25 °C) on ice and with buffers at +4 °C. The plates were incubated overnight at +4 °C (15−20 h). The incubation was stopped by filtration through GF/B filter on a Tomtec Cell-Harvester. The GF/B filters were dried for at least 1 h at 65 °C. A MeltiLex scintillation wax was melted onto filters with the Microsealer. Filters were placed in a sample bag, which was thereafter trimmed with scissors to fit the filter cassette. The cassette were placed in the Microbeta and measured for 1 min/position, returning ccpm (corrected counts per minute). For compounds able to displace ^{3}(H)-dexamethasone from the receptor, an IC_{50} value (the concentration required to inhibit 50% of the binding of ^{3}(H)-dex) was determined by a nonlinear four-parameter logistic model:

$$b = ((b_{max} - b_{min})/(1 + (I/IC_{50})^S)) + b_{min}I$$

where I is the added concentration of binding inhibitor, IC_{50} is the concentration for inhibitor at half-maximal binding, and S is a slope factor. For determinations of the concentration of ^{3}H-dex in the solutions, regular scintillation counting in a Wallac Rackbeta 1214 was performed using the scintillation cocktail Supermix (Wallac). The Microbeta instrument generates the mean cpm (counts per minute) value/minute and corrects for individual variations between the detectors, thus generating corrected cpm values. Counting efficiency between detectors differed by less than 5%. Similar protocols were employed to measure affinity of the compounds for progest-

erone receptor (PR), mineralocorticoid receptor (MR), androgen receptor (AR), estrogen receptors (ERα and ERβ), and thyroid hormone receptors (TRα and TRβ). IC_{50} values were converted to K_i using the standard equation

$$K_i = IC_{50}/(1 + [ref]/K_d(ref))$$

where ref is the reference radioligand

GRAF Assay. Chinese hamster ovarian cells (CHO-K1) were stably transfected with an expression plasmid encoding hGR and a reporter construct containing a glucocortiocoid response element driving expression of alkaline phosphatase (ALP) to produce the GRAF cell line. GRAF cells were grown in HAM's F12 media supplemented with 10% FCS and 1% L-glutamine. Induction media was Opti-MEM with 1% L-glutamine, 50 μg/mL gentamycin. GRAF cells were seeded in growth medium in 96-well plates at ∼50 000 cells per well. After 24 h of incubation, the cells were induced with test compounds as well as dexamethasone, as a positive control, at serial dilutions, to measure agonist response. To examine antagonist effects GRAF cells were treated with increasing amounts of test compounds in the presence of 5 nM dexamethasone. After 48 h of induction, disodium 3-(4-methoxy-spiro{1,2-dioxetane-,2′-(5′-chloro)tricyclo[3.3.1.13.7]decan}-4-yl)phenyl phosphate (CSPD; Applied Biosystems) was added to the medium, and levels of secreted alkaline phosphatase were analyzed by chemiluminescence on a MicroBeta Trilux.

Hepatocyte TAT Assay. Primary rat hepatocytes were plated in 96-well collagen-coated plates at 50 000 cells per well. Cells were incubated in DMEM with 10% charcoal-stripped serum at 37 °C for 4 h. Cells were pretreated with serial diluted compounds for 30 min, followed by 100 nM of prednisolone for 4 h. Cells were then washed with PBS and lysed with lysis buffer (50 mM Tris-HCl, pH 7.5, 0.1 mM EDTA, 10 μg/mL PMSF, and 0.1% Lubrol PX). The tyrosine aminotransferase assay was performed according to standard protocols.[34] Basically, the substrate mixture containing 6 mM L-tyrosine, 11 μM α-ketoglutarate, and 56 μM pyridoxal-5′ phosphate in potassium phosphate buffer was added to the lysates and incubated for 30 min at 37 °C. The reaction was stopped by 10 N KOH and plates were read on a Spectrophotometer at 340 nm. Wells that contained substrate without compound or Dex were used as the background, while the wells that contained substrate and Dex without any compound were considered as maximal signal. Percent inhibition of each compound was calculated relative to the maximal signal, and IC_{50} curves were generated.

In Vivo Compound Evaluation. All protocols involving animals were approved in advance by the Abbott Institutional Animal Care and Use Committee (IACUC). All in vivo data were analyzed for statistical significance (two-tailed *t* test) using GraphPad Instat. Drug-treated groups were compared to vehicle controls at the same day or time point.

Rat Prednisolone Challenge Model. Overnight fasted 150 g male Sprague Dawley rats are orally dosed with vehicle, RU-486 (30−100 mg/kg), or selected glucocorticoid receptor antagonists (30−100 mg/kg), 60 min prior to an oral challenge with prednisolone at 10 mg/kg. Six hours following the prednisolone challenge, rats are euthanized with CO_2, and bled via cardiac puncture for evaluation of blood lymphocytes and plasma drug levels. 7 mm liver biopsy punches are harvested for evaluation of tyrosine aminotransferase (TAT), hepatic glycogen, and GR antagonist levels. Additional liver tissue, retroperitoneal fat, skeletal muscle, kidney, and skin from an ear biopsy are also removed for isolation and evaluation of mRNA. Prednisolone increases hepatic TAT and glycogen levels and induces severe lymphopenia during the 6 h challenge interval. At doses of 100 mg/kg, RU-486 completely antagonizes these hepatic and peripheral responses.

Mouse Hypothalamic−Pituitary−Adrenal (HPA) Activation Model. Nonfasted CD-1 male mice, weighing approximately 25 g, are dosed with vehicle, RU-486 (30−100 mg/kg), or GR antagonist (30−100 mg/kg) at 0800 h when corticosterone levels are low. Two hours later, mice are euthanized with CO_2 and bled by cardiac puncture, and plasma is analyzed for corticosterone by mass spectroscopy and for adrenocorticotropic hormone (ACTH) levels by ELISA. Brains and plasma are also removed for analysis of GR antagonist levels. At doses of 100 mg/kg, RU-486 significantly increases ACTH and corticosterone levels compared to vehicle controls.

Acknowledgment. The authors thank Peter Agback of KaroBio, and the Abbott Analytical Department, for assistance in acquiring ^{1}H-NMR and mass spectra. We note the valuable contributions of Bryan Sorensen to the synthesis of intermediates such as **11**, and greatly appreciate the efforts of Rob Kimura and David Beno to study A-348441 in the chronically catheterized rat model.

References

(1) van den Berghe, G. Disorders of gluconeogenesis. *J. Inherit. Metab. Dis.* **1996**, *19(4)*, 470−477.
(2) Rallison, M. L.; Meikle, A. W.; Zigrang, W. D. Hypoglycemia and lactic acidosis associated with fructose-1,6-diphosphatase deficiency. *J. Pediatr.* **1979**, *94(6)*, 933−936.
(3) Friedman, J. E.; Sun, Y.; Ishizuka, T.; Farrell, C. J.; McCormack, S. E.; Herron, L. M.; Hakimi, P.; Lechner, P.; Yun, J. S. Phosphoenolpyruvate carboxykinase (GTP) gene transcription and hyperglycemia are regulated by glucocorticoids in genetically obese *db/db* transgenic mice. *J. Biol. Chem.* **1997**, *272(50)*, 31475−31481.
(4) Baxter, J. D. Glucocorticoid hormone action. *Pharmacol. Ther. [B]* **1976**, *2(3)*, 605−669.
(5) Nieman, L. K.; Chrousos, G. P.; Kellner, C.; Spitz, I. M.; Nisula, B. C.; Cutler, G. B.; Merriam, G. R.; Bardin, C. W.; Loriaux, D. L. Successful treatment of Cushing's syndrome with the glucocorticoid antagonist RU 486. *J. Clin. Endocrinol. Metab.* **1985**, *61(3)*, 536−540.
(6) Chu, J. W.; Matthias, D. F.; Belanoff, J.; Schatzberg, A.; Hoffman, A. R.; Feldman, D. Successful long-term treatment of refractory Cushing's disease with high-dose mifepristone (RU 486). *J. Clin. Endocrinol. Metab.* **2001**, *86(8)*, 3568−3572.
(7) Armstrong, L.; Bell, P. M. Addison's disease presenting as reduced insulin requirement in insulin-dependent diabetes. *Br. Med. J.* **1996**, *312(7046)*, 1601−1602.
(8) Gettys, T. W.; Watson, P. M.; Taylor, I. L.; Collins, S. RU-486 (mifepristone) ameliorates diabetes but does not correct deficient beta-adrenergic signaling in adipocytes from mature C57BL/6J-*ob/ob* mice. *Int. J. Obes. Relat. Metab. Disord.* **1997**, *21(10)*, 865−873.
(9) Garrel, D. R.; Moussali, R.; De Oliveira, A.; Lesiege, D.; Lariviere, F. RU 486 prevents the acute effects of cortisol on glucose and leucine metabolism. *J. Clin. Endocrinol. Metab.* **1995**, *80(2)*, 379−385.
(10) Lamberts, S. W.; Koper, J. W.; deJong, F. H. The endocrine effects of long-term treatment with mifepristone (RU 486). *J. Clin. Endocrinol. Metab.* **1991**, *73(1)*, 187−191.
(11) Leeson, P. D.; Emmett, J. C.; Shah, V. P.; Showell, G. A.; Novelli, R.; Prain, H. D.; Benson, M. G.; Ellis, D.; Pierce, N. J.; Underwood, A. H. Selective thyromimetics. Cardiac-sparing thyroid hormone analogues containing 3′-arylmethyl substituents. *J. Med. Chem.* **1989**, *32*, 2(2), 320−336.
(12) Nezasa, K.-I.; Higaki, K.; Matsumura, T.; Inazawa, K.; Hasegawa, H.; Nakano, M.; Koike, M. Liver-specific distribution of rosuvastatin in rats: Comparison with pravastatin and simvastatin. *Drug Metab. Distr.* **2002**, *30(11)*, 1158−1163.
(13) Biessen, E. A. L.; Beuting, D. M.; Roelen, H. C. P. F.; van de Marel, G. A.; van Boom, J. H.; van Berkel, T. J. C. Synthesis of cluster galactosides with high affinity for the hepatic asialoglycoprotein receptor. *J. Med. Chem.* **1995**, *38(9)*, 1538−1546.
(14) Lu, X.; Fischman, A. J.; Jyawook, S. L.; Hendricks, K.; Tompkins, R. G.; Yarmush, M. L. Antisense DNA delivery in vivo: liver targeting by receptor-mediated uptake. *J. Nucl. Med.* **1994**, *35-(2)*, 269−75.
(15) Beljaars, L.; Melgert, B. N.; Meijer, D. K. F.; Molema, G.; Poelstra, K. Neoglyco- and neopeptide albumins for cell-specific delivery of drugs to chronically diseased livers. *Drugs Pharm. Sci.* **2001**, *115(Drug Targeting Technology)*, 189−240.
(16) Hatori, Y.; Kawakami, S.; Yamashita, F.; Hashida, M. Controlled biodistribution of galactosylated liposomes and incorporated probucol in hepatocyte-selective drug targeting. *J. Controlled Release* **2000**, *69*, 369−377.
(17) Bebernitz, G. R.; Dain, J. G.; Deems, R. O.; Otero, D. A.; Simpson, W. R.; Strohschein, R. J. Reduction in glucose levels in STZ Diabetic Rats by 4-(2,2-dimethyl-1-oxopropyl)benzoic acid: A prodrug approach for targeting the liver. *J. Med. Chem.* **2001**, *44*, 512−523.

(18) Carey, M. C.; Cahalane, M. J. Enterohepatic Circulation. In *The Liver: Biology and Pathobiology*, 2nd ed.; Raven Press: Ltd, New York, 1988; Chapter 33, pp 573−616. Data derived from other referenced sources.
(19) Wess, G.; Kramer, W.; Bartmann, W.; Enhsen, A.; Glombik, H.; Müllner, S.; Bock, K.; Dries, A.; Kleine, H.; Schmitt, W. Modified bile acids: Preparation of 7α, 12α-dihydroxy-3*β*- and 7α, 12α-dihydroxy-3α-(2-hydroxyethoxy)-5*β*-cholanic acid and their biological activity. *Tetrahedron Lett.* **1992**, *33(2)*, 195−198.
(20) Kullak-Ublik, G.-A.; Glasa, J.; Boker, C.; Oswald, M.; Grutzner, U.; Hagenbuch, B.; Stieger, B.; Meier, P. J.; Beuers, U.; Kramer, W.; Wess, G.; Paumgartner, G. Chlorambucil-taurocholate is transported by bile acid carriers expressed in human hepatocellular carcinomas. *Gastroenterology* **1997**, *113*, 1295−1305.
(21) Starke, D.; Lischka, K.; Pagels, P.; Uhlmann, E.; Kramer, W.; Wess, G.; Petzinger, E. Bile acid-oligodeoxynucleotide conjugates: Synthesis and liver excretion in rats. *Bioorg. Med. Chem. Lett.* **2001**, *11*, 945−949.
(22) Kramer, W.; Wess, G.; Schubert, G.; Bickel, M.; Girbig, F.; Gutjahr, U.; Kowalewski, S.; Baringhaus, K.-H.; Enhsen, A.; Glombik, H.; Müllner, S.; Neckermann, G.; Schulz, S.; Petzinger, E. Liver-specific drug targeting by coupling to bile acids. *J. Biol. Chem.* **1992**, *267(26)*, 18598−18604. *See also* Holzinger, F.; Schteingart, C. D.; Ton-Nu, H.-T.; Eming, S. A.; Monte, M. J.; Hagey, L. R.; Hofman, A. F. Fluorescent bile acid derivatives: Relationship between chemical structure and hepatic and intestinal transport in the rat. *Hepatology* **1997**, *26(3)*, 1263−1271.
(23) Kim, D.-C.; Harrison, A. W.; Ruwart, M. J.; Wilkinson, K. F.; Fisher, J. F.; Hidalgo, I. J.; Borchardt, R. T. Evaluation of the bile acid transporter in enhancing intestinal permeability to renin-inhibitory peptides. *J. Drug Targeting* **1993**, *1*, 347−359.
(24) Acosta, K.; Cessac, J. W.; Rao, N.; Kim, H. K. Oxidative demethylation of 4-substituted *N*, *N*-dimethylanilines with iodine and calcium oxide in the presence of methanol. *J. Chem. Soc. Chem. Commun.* **1994**, 1985−1986.
(25) Hagberg, L.; Apelqvist, T. Manuscript in preparation.
(26) Tserng, K.-Y. A convenient synthesis of 3-keto bile acids by selective oxidation of bile acids with silver carbonate-Celite. *J. Lipid Res.* **1978**, *19(4)*, 501−504.
(27) Kauppi, B.; Jakob, C.; Färnegårdh, M.; Yang, J.; Ahola, H.; Alarcon, M.; Calles, K.; Engström, O.; Harlan, J.; Muchmore, S.; Ramqvist, A.-K.; Thorell, S.; Öhman, L.; Greer, J.; Gustafsson, J.-Å.; Carlstedt-Duke, J.; Carlquist, M. The three-dimensional structures of antagonistic and agonistic forms of the glucocorticoid receptor ligand-binding domain: RU-486 induces a transconformation that leads to active antagonism. *J. Biol. Chem.* **2003**, *278(25)*, 22748−22754.
(28) Williams, S. P.; Sigler, P. B. Atomic structure of progesterone complexed with its receptor. *Nature* **1998**, *393*, 392−396.
(29) Crofford, O. B. Diabetes Control and Complications. *Annu. Rev. Med.* **1995**, *46*, 267−279.
(30) Jover, E.; Paradinas, C.; Prieto, J.; Arranz, M. T.; Para, J.; Velasco, R. Study of the effect of ACTH and cortisol on the plasma lipids in man using thin-layer chromatography. *J. Med.* **1976**, *7(2)*, 131−142.
(31) The hepatic selectivity of A-348441 also reduces its ability to block peripheral progesterone receptors. We have determined (P. Jacobson et al., manuscript in preparation) that A-348441 is much less effective than mifepristone in a mouse anti-progestin model.
(32) Osterlund, M.; Barkhem, T., et al. Manuscript in preparation.
(33) Studies performed by R. Kimura and D. Beno using a chronically catheterized rat model; data not shown here.
(34) Granner, D. K.; Tomkins, G. M. Tyrosine Aminotransferase (Rat Liver). *Methodology* **1970**, *17A*, 633−637.

JM0400045